Printed Periodic Waveguide Structures: Full-wave characterization, Guided-wave characteristics and Applications

R. S. Kshetrimayum

Microwave Lab, Indian Institute of Science, Bangalore

Presentation in a Nutshell

1. Full-wave characterization
   - Hybrid MoM-Immittance Approach
   - Impedance-type for printed strip
   - Admittance-type for printed slot
2. Guided-wave characteristics
   - Complex propagation constant & wave impedance
   - FSS strip printed periodic waveguide
   - FSS slot printed periodic waveguide
3. Applications
   - SIS resonator waveguide filters
   - EBG/PBG structures
   - Metamaterials Architecture

Section 1

Full-wave characterization

MoM

- In electromagnetics, some problems formulated as complex integral equations (Lu=f)
- Have no analytical solutions and therefore must be solved numerically.
- MoM transforms such integral equations into matrix systems of linear equations (Ax=b)
- Advantages over FEM, FDTD, etc. are MoM uses surface discretization. Hence needs less CPU time and memory.

Immittance Approach

- Simple method for formulating spectral domain dyadic Green's functions
- By drawing equivalent TE and TM circuit models
- Very efficient for analyzing multilayered structures

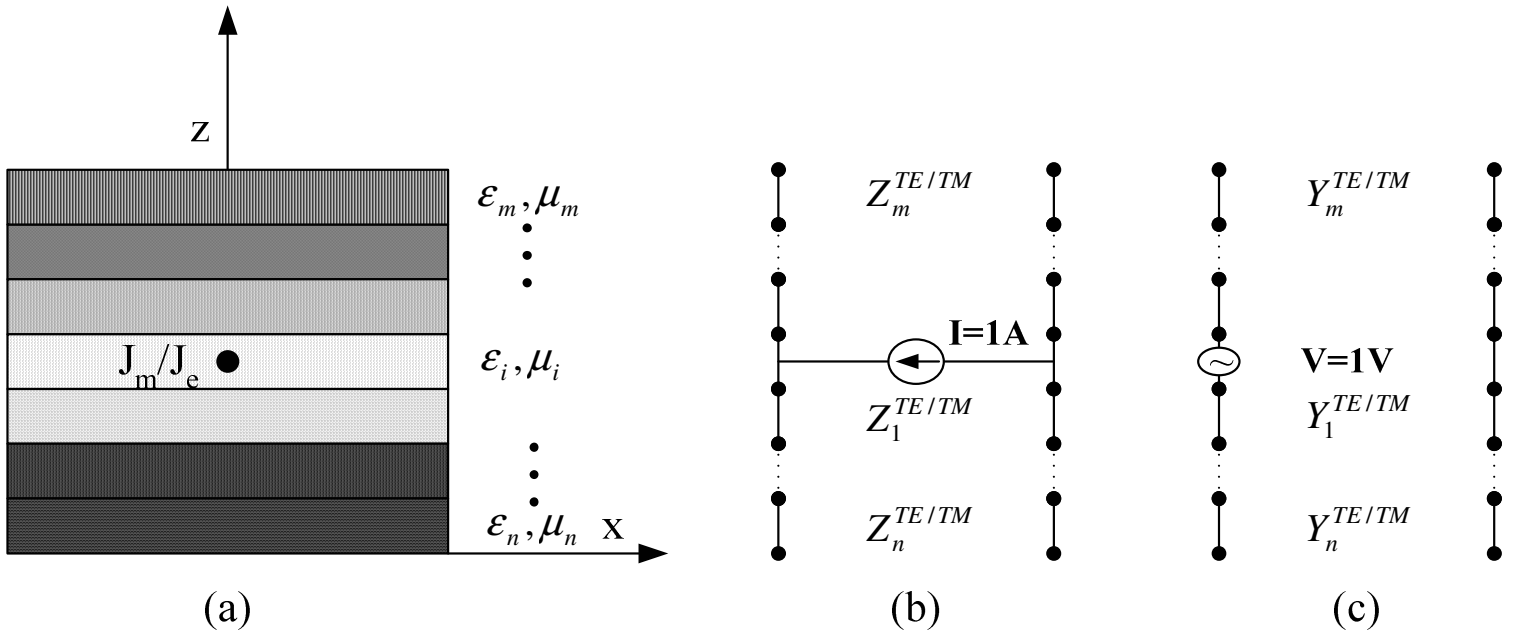

(a) (b) (c)

Hybrid MoM-Immittance Approach (HMIA)

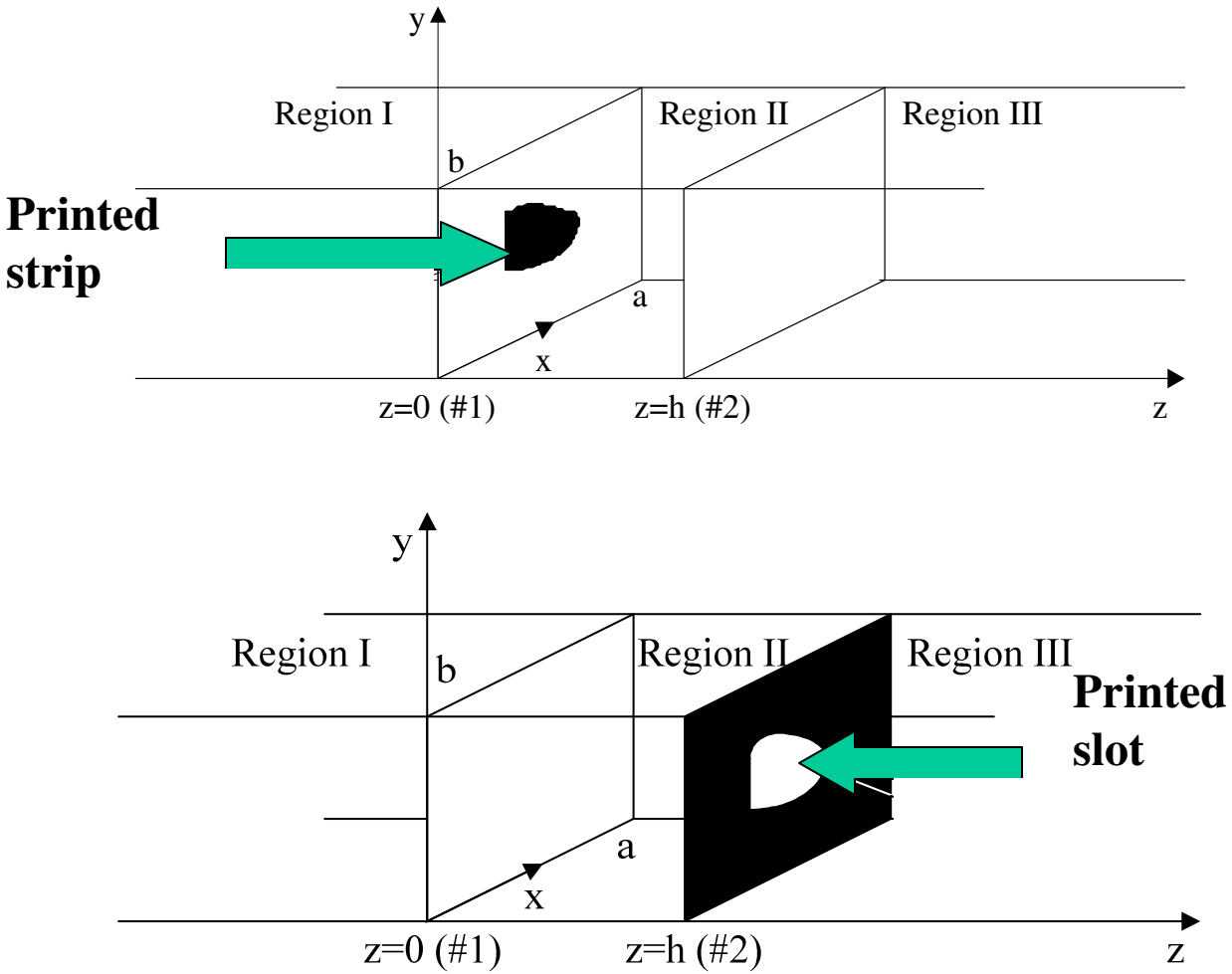

Impedance-type HMIA for printed strip

1. Electric Field Integral Equation (EFIE)

- total tangential incident and scattered electric field at the interface is zero
- scattered electric field expressed in terms of electric dyadic Green's function and unknown electric current density on printed strip
- unprimed coordinates represent observation point whereas source location is represented by primed coordinates

$$\hat{z} \times (\overline{E}^{\,inc}(\overline{r}) + \overline{E}^{\,scatt}(\overline{r})) = 0$$

$$\hat{z} \times (\overline{E}^{\,inc}(\overline{r}) + \int_{strip} \overline{\overline{G}}_{EJ}(\overline{r}, \overline{r}').\overline{J}(\overline{r}')d\overline{S}') = 0$$

Impedance-type HMIA for printed strip

2. Impedance-type HMIA Matrix

$$\begin{bmatrix} [Zxx] & [Zxy] \\ [Zyx] & [Zyy] \end{bmatrix} \begin{bmatrix} [Ix] \\ [Iy] \end{bmatrix} = \begin{bmatrix} [Vx] \\ [Vy] \end{bmatrix}$$

Voltage matrices

Impedance matrices

Current matrices

$$z_{xx}(m,n) = -\sum_{m=0}^{M+1}\sum_{n=0}^{N+1} \tilde{T}_x^*(k_{xm},k_{yn})\tilde{G}_{EJ}^{xx}(k_{xm},k_{yn})\tilde{B}_x(k_{xm},k_{yn})$$

$$z_{xy}(m,n) = -\sum_{m=0}^{M+1}\sum_{n=0}^{N+1} \tilde{T}_x^*(k_{xm},k_{yn})\tilde{G}_{EJ}^{xy}(k_{xm},k_{yn})\tilde{B}_y(k_{xm},k_{yn})$$

$$z_{yx}(m,n) = -\sum_{m=0}^{M+1}\sum_{n=0}^{N+1} \tilde{T}_y^*(k_{xm},k_{yn})\tilde{G}_{EJ}^{yx}(k_{xm},k_{yn})\tilde{B}_x(k_{xm},k_{yn})$$

$$z_{yy}(m,n) = -\sum_{m=0}^{M+1}\sum_{n=0}^{N+1} \tilde{T}_y^*(k_{xm},k_{yn})\tilde{G}_{EJ}^{yy}(k_{xm},k_{yn})\tilde{B}_y(k_{xm},k_{yn})$$

Impedance-type HMIA for printed strip

2. Impedance-type HMIA Matrix (Contd.)

$$v_x = \iint_{strip} T_x^*(x,y) E_x^{inc}(x,y) dxdy$$

$$v_y = \iint_{strip} T_y^*(x,y) E_y^{inc}(x,y) dxdy$$

- Impedance sub-matrix denotes the x-directed testing of electric field produced by y-directed current basis elements
- Voltage sub-matrices refer to x- and y-directed testing of incident electric field.
- Current sub-matrices are respectively the unknown electric current expansion coefficients associated with x-directed and y-directed basis function
- Once we know the unknown current matrices, we can get the scattering parameters from the EFIE.

Admittance-type HMIA for printed slot

1. Magnetic Field Integral Equation (MFIE)

- tangential continuity of the total magnetic field, which consists of incident and scattered magnetic field, on printed slot.
- scattered magnetic field can be expressed in terms of magnetic dyadic Green's functions, and magnetic current density, over printed slot.

$$\hat{z} \times (\overline{H}^{inc}(\bar{r}) + \overline{H}^{scatt}(\bar{r}))\Big|_{z=0^-} = \hat{z} \times (\overline{H}^{scatt}(\bar{r}))\Big|_{z=0^+}$$

$$-\hat{z} \times \overline{H}^{inc}(\bar{r}) = \int_{slot} \overline{\overline{G}}^{-}_{HM}(\bar{r}, \bar{r}').\overline{M}(\bar{r}')d\overline{S}' + \int_{slot} \overline{\overline{G}}^{+}_{HM}(\bar{r}, \bar{r}').\overline{M}(\bar{r}')d\overline{S}')$$

Impedance-type HMIA for printed slot

2. Admittance-type HMIA Matrix

$$\begin{bmatrix} [Yxx] & [Yxy] \\ [Yyx] & [Yyy] \end{bmatrix} \begin{bmatrix} [Vx] \\ [Vy] \end{bmatrix} = \begin{bmatrix} [Ix] \\ [Iy] \end{bmatrix}$$

Admittance matrices

Voltage matrices

Current matrices

$$y_{xx}(m,n) = -\sum_{m=0}^{M+1}\sum_{n=0}^{N+1} \tilde{T}_x^*(k_{xm},k_{yn})\tilde{G}_{HM}^{xx}(k_{xm},k_{yn})\tilde{B}_x(k_{xm},k_{yn})$$

$$y_{xy}(m,n) = -\sum_{m=0}^{M+1}\sum_{n=0}^{N+1} \tilde{T}_x^*(k_{xm},k_{yn})\tilde{G}_{HM}^{xy}(k_{xm},k_{yn})\tilde{B}_y(k_{xm},k_{yn})$$

$$y_{yx}(m,n) = -\sum_{m=0}^{M+1}\sum_{n=0}^{N+1} \tilde{T}_y^*(k_{xm},k_{yn})\tilde{G}_{HM}^{yx}(k_{xm},k_{yn})\tilde{B}_x(k_{xm},k_{yn})$$

$$y_{yy}(m,n) = -\sum_{m=0}^{M+1}\sum_{n=0}^{N+1} \tilde{T}_y^*(k_{xm},k_{yn})\tilde{G}_{HM}^{yy}(k_{xm},k_{yn})\tilde{B}_y(k_{xm},k_{yn})$$

Admittance-type HMIA for printed slot

2. Admittance-type HMIA Matrix (Contd.)

$$i_x = \iint_{slot} T_x^*(x,y) H_x^{inc}(x,y)\,dxdy$$

$$i_y = \iint_{slot} T_y^*(x,y) H_y^{inc}(x,y)\,dxdy$$

- Admittance sub-matrix denotes x-directed testing of incident magnetic field produced by y-directed magnetic current basis elements.
- Current sub-matrices refer to x- and y-directed testing of incident magnetic field.
- Voltage sub-matrices are respectively the unknown magnetic voltage expansion coefficients associated with x-directed and y-directed basis functions
- Once we know the unknown current matrices, we can get the scattering parameters from the MFIE.

Equivalent Circuit Parameter Extraction

- For lossless networks, impedance or admittance elements are purely imaginary.
- Equivalent circuit parameters from the sign of impedance or admittance elements in the two-port equivalent network.

$$Z_a = \frac{A-1}{C} \qquad Z_b = \frac{D-1}{C} \qquad Z_c = \frac{1}{C}$$

$$Y_a = \frac{1}{B} \qquad Y_b = \frac{A-1}{B} \qquad Y_c = \frac{D-1}{B}$$

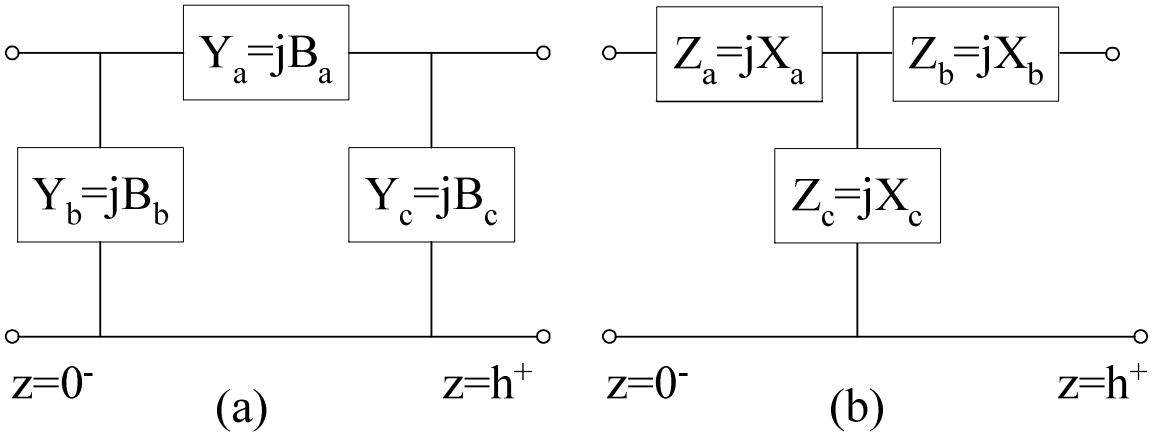

Equivalent circuit for printed strip

Normalized X_b versus frequency

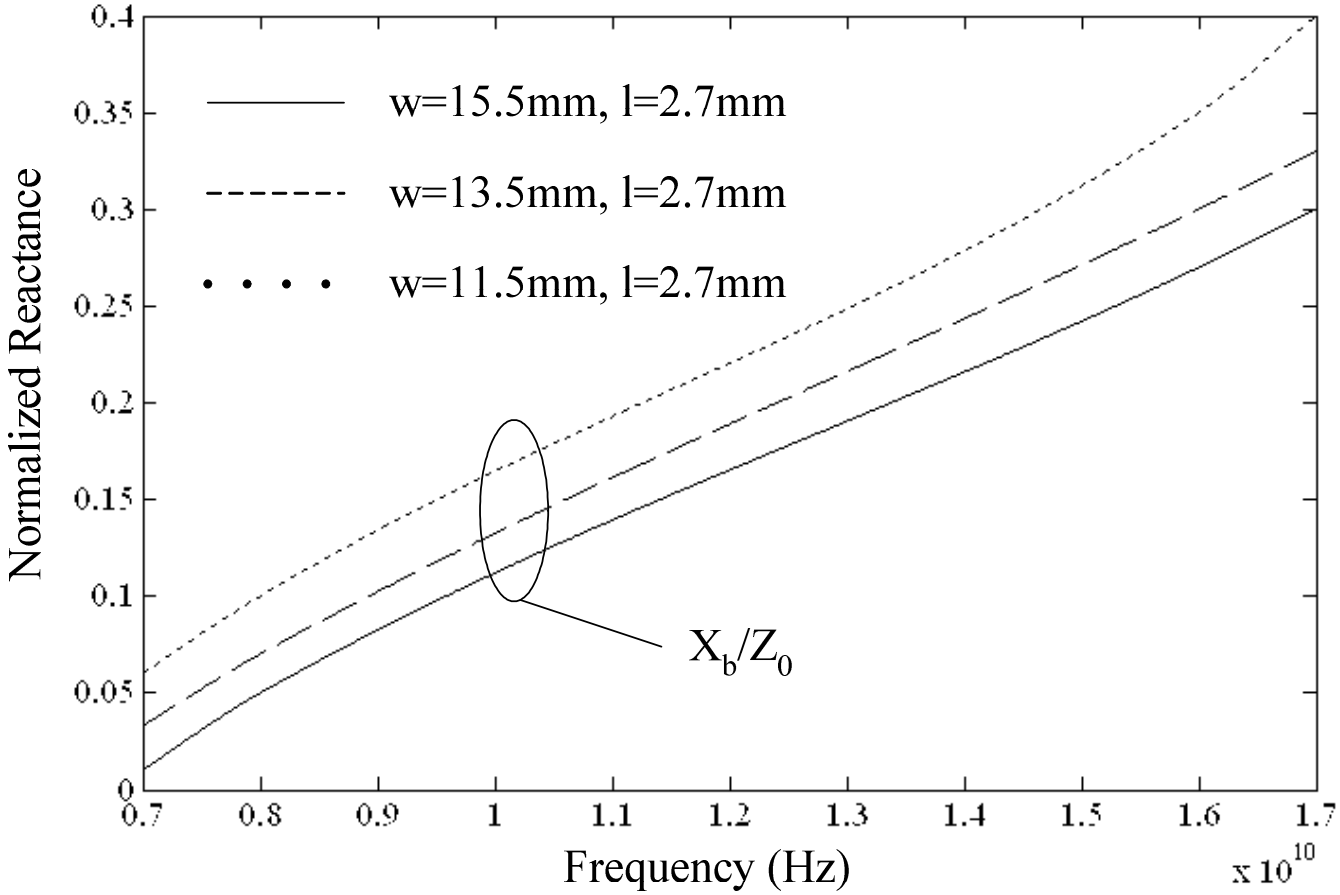

Equivalent circuit for printed strip

Normalized X_c versus frequency

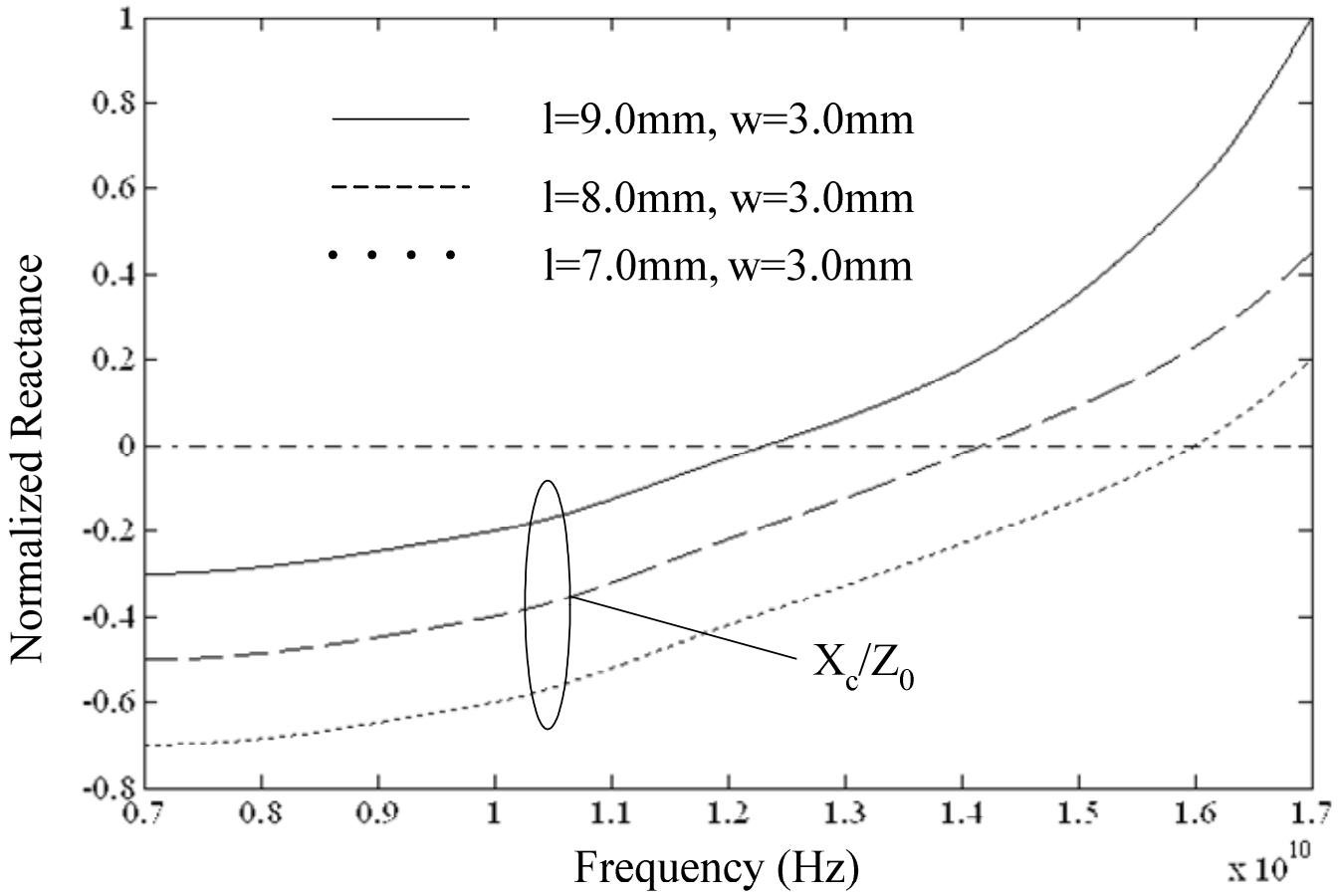

Equivalent circuit for printed strip

Normalized X_a is very small and can be neglected in the equivalent T-network. Hence the equivalent circuit is as shown in Figure below. Similarly, we can get the equivalent circuit for the printed slot from the Z parameters of the T-network.

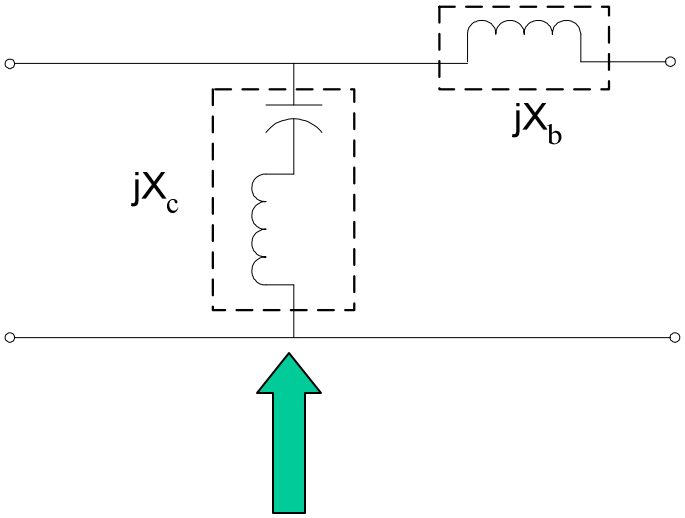

Eq. Ckt. for printed strip

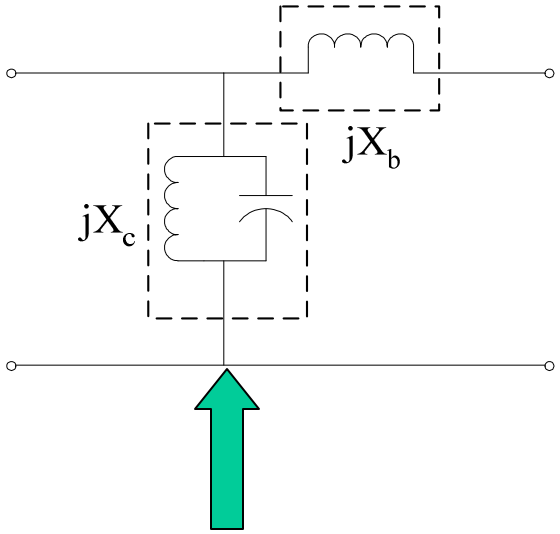

Eq. Ckt. for printed slot

Section 2

Guided-wave characteristics

Guided-wave characteristics

- Constitutes complex propagation constant ($\gamma=\alpha+j\beta$) and complex wave impedance ($Z_0=\mathrm{Re}(Z_0)+j\mathrm{Im}(Z_0)$)
- Can be obtained from the ABCD parameters of a unit cell
- Assumption: periodicity of the periodic structures is chosen such that all higher order evanescent modes excited by the waveguide discontinuity have decayed to a negligible value at the next consecutive discontinuities

Propagation $$\cos \beta p = \frac{A_u + D_u}{2}$$

Attenuation $$\cosh \alpha p = \frac{A_u + D_u}{2}$$

$$\frac{Z}{Z_0} = \pm\sqrt{\frac{B}{C}}$$

FSS strip printed periodic waveguide

- 3-D geometry of an infinite-extended waveguide based periodic structure loaded with any arbitrary FSS strip layers.
- Periodicity p of printed periodic waveguide structure is chosen as 4.00mm.
- X-band waveguide (a=22.86mm and b=10.16mm)

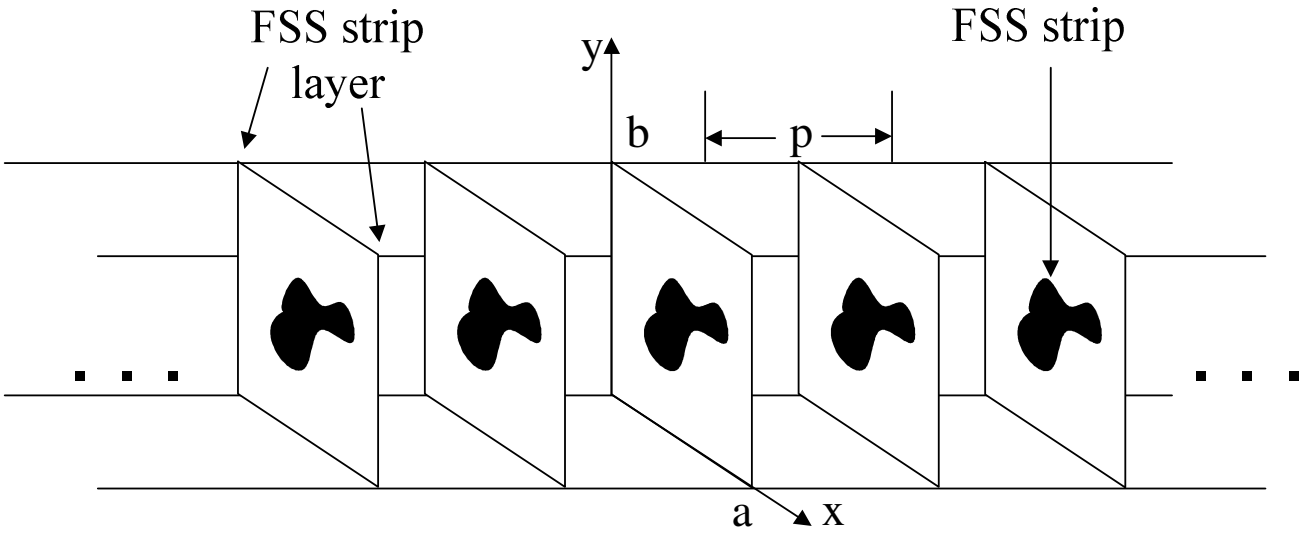

Important terms

- Phase velocity of a wave is the rate at which phase of wave propagates in space
- The group velocity of a wave is the velocity with which the overall shape of wave amplitude
- The phase velocity is also given by the slope of a line from origin to a point on dispersion curve, while the group velocity is given by slope of a tangent to the dispersion curve.
- Forward and backward wave
- Slow wave ($\beta/k_0>1$) and fast wave ($\beta/k_0<1$)

$$v_p = \frac{\omega}{k} \qquad v_g = \frac{\partial \omega}{\partial k}$$

Square Loop FSS strip printed periodic waveguide

dimensions of strip are chosen as l_1=7.0mm, l_2=7.00mm and w_1=2.00mm

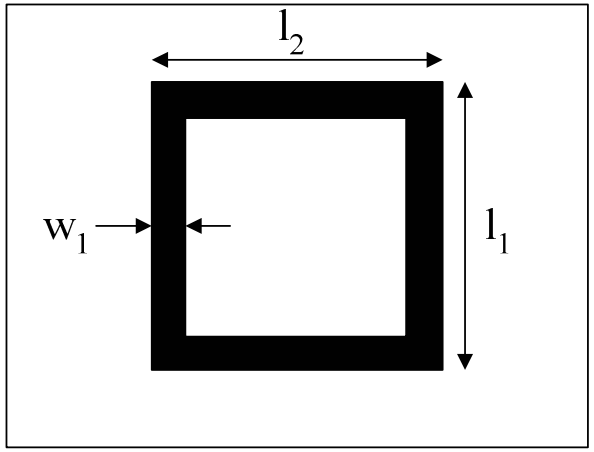

Square Loop FSS strip printed periodic waveguide

Normalized propagation constant ($\gamma/k_0=\alpha/k_0+j\beta/k_0$)

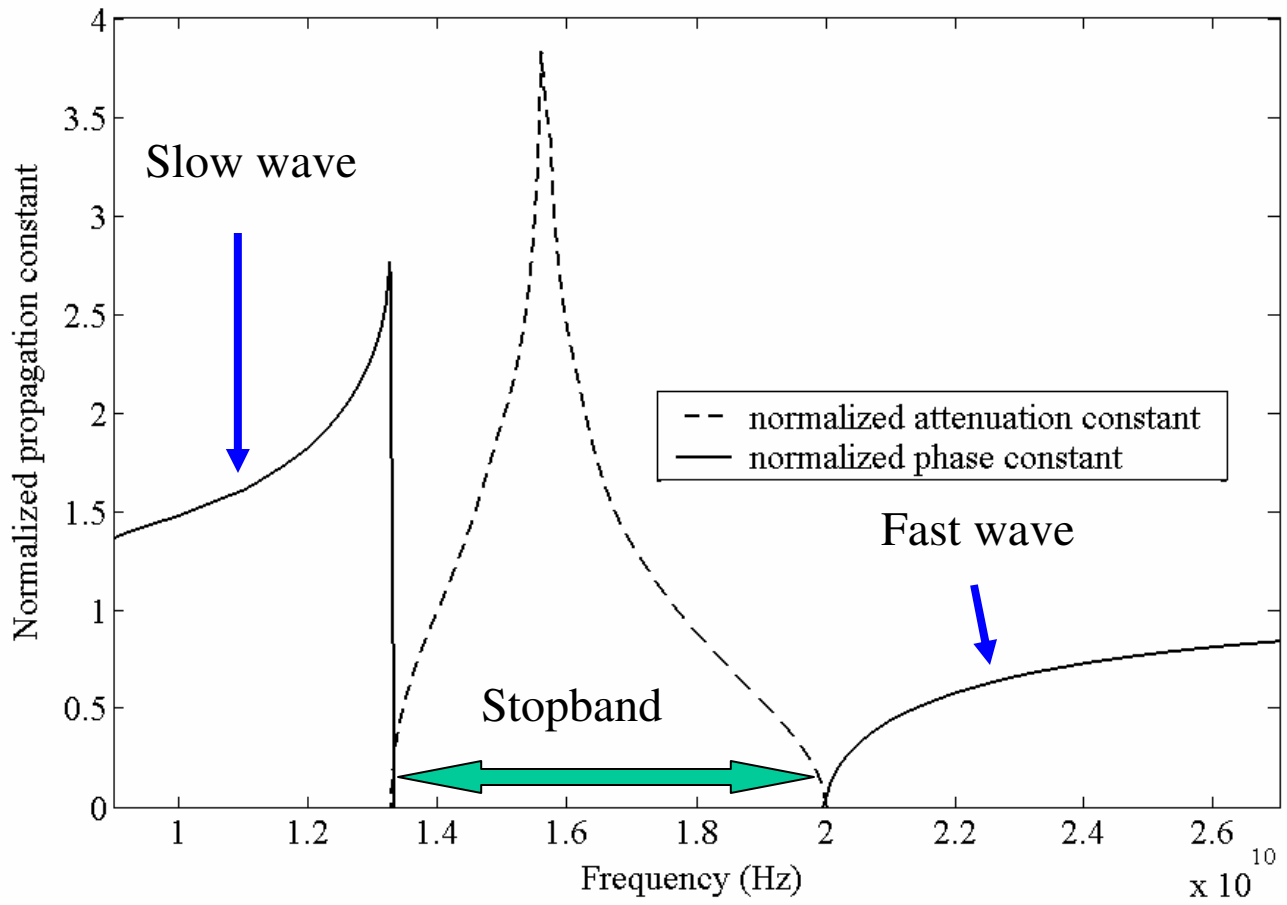

Square Loop FSS strip printed periodic waveguide

Normalized wave impedance (Z/Z_0)

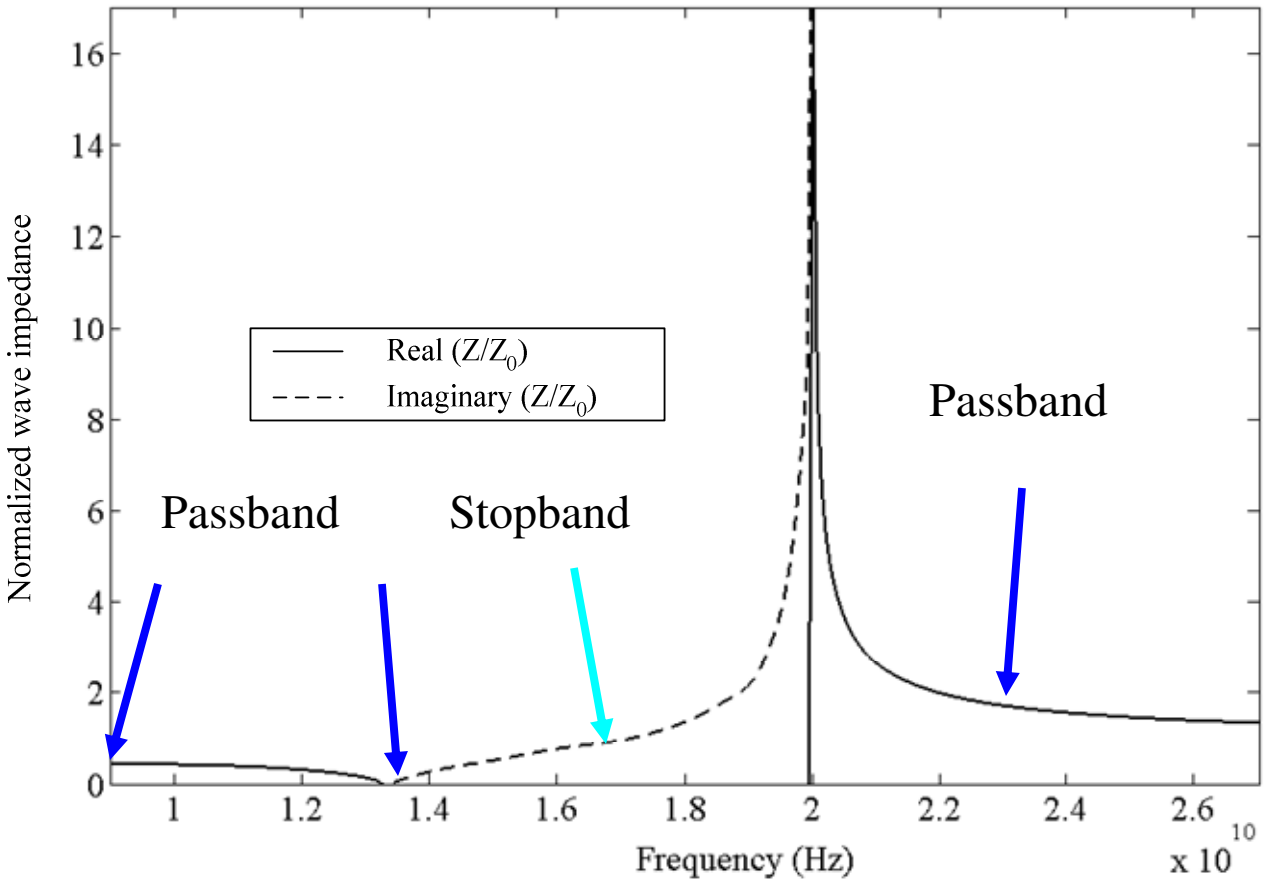

Jerusalem Cross FSS strip printed periodic waveguide

l_1=7.0mm, l_2=7.00mm, l_3=3.50mm, w_1=2.00mm, w_2=2.00mm and w_3=1.00mm.

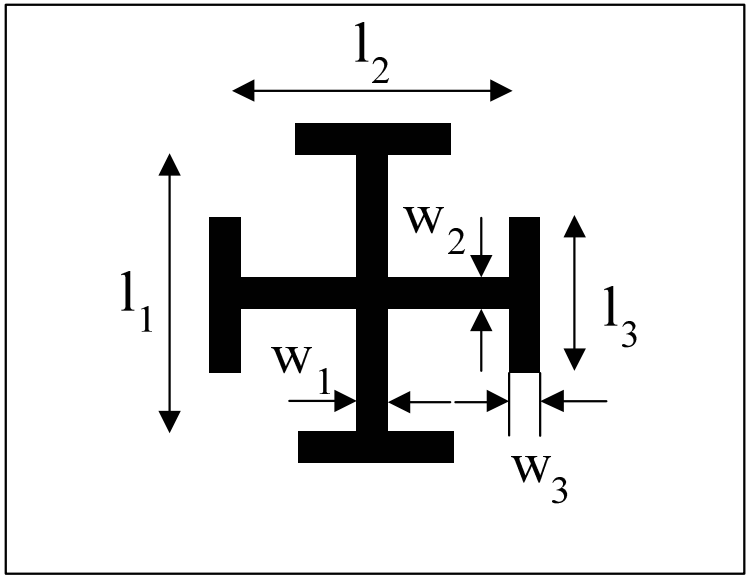

Square Loop FSS strip printed periodic waveguide

Normalized propagation constant ($\gamma/k_0=\alpha/k_0+j\beta/k_0$)

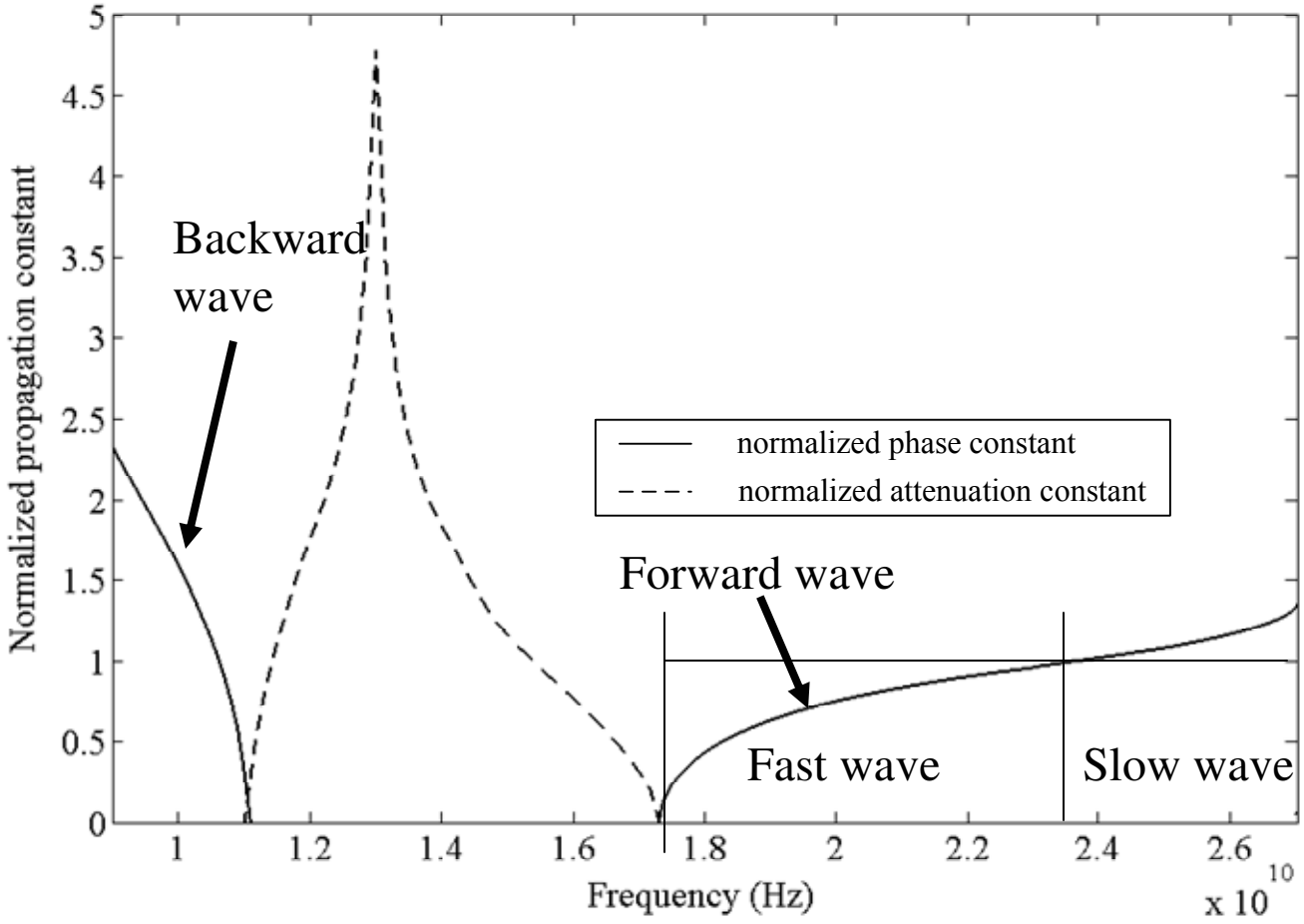

Square Loop FSS strip printed periodic waveguide

Normalized wave impedance (Z/Z_0)

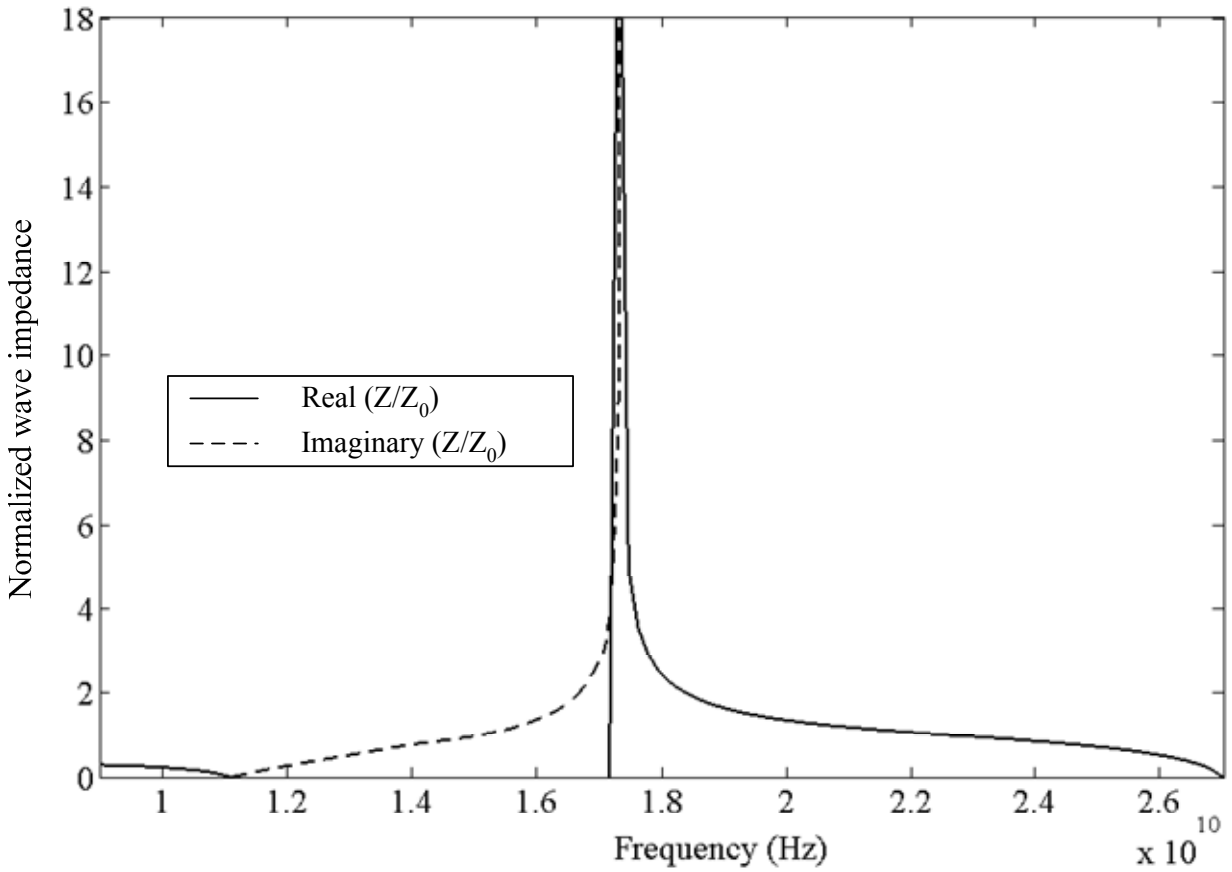

FSS slot printed periodic waveguide

3-D geometry of an infinite-extended waveguide based periodic structure loaded with any arbitrary FSS slot layers.

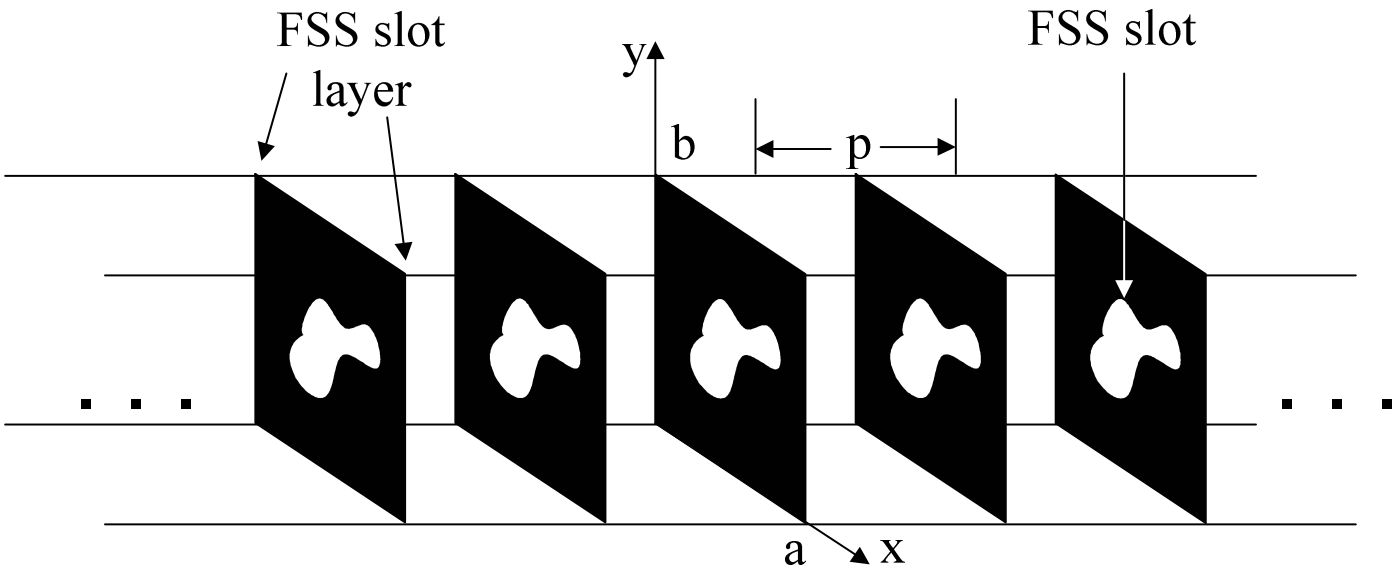

Ring FSS slot printed periodic waveguide

r_1=4.5mm and r_2=1.5mm

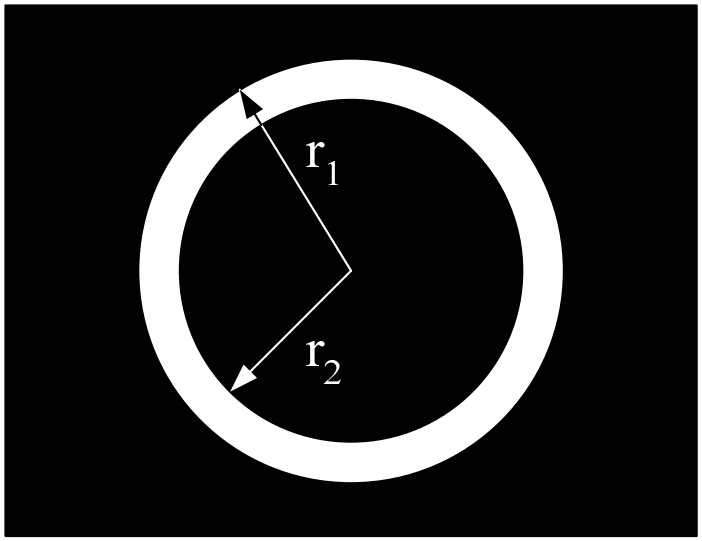

Square Loop FSS strip printed periodic waveguide

Normalized propagation constant ($\gamma/k_0=\alpha/k_0+j\beta/k_0$)

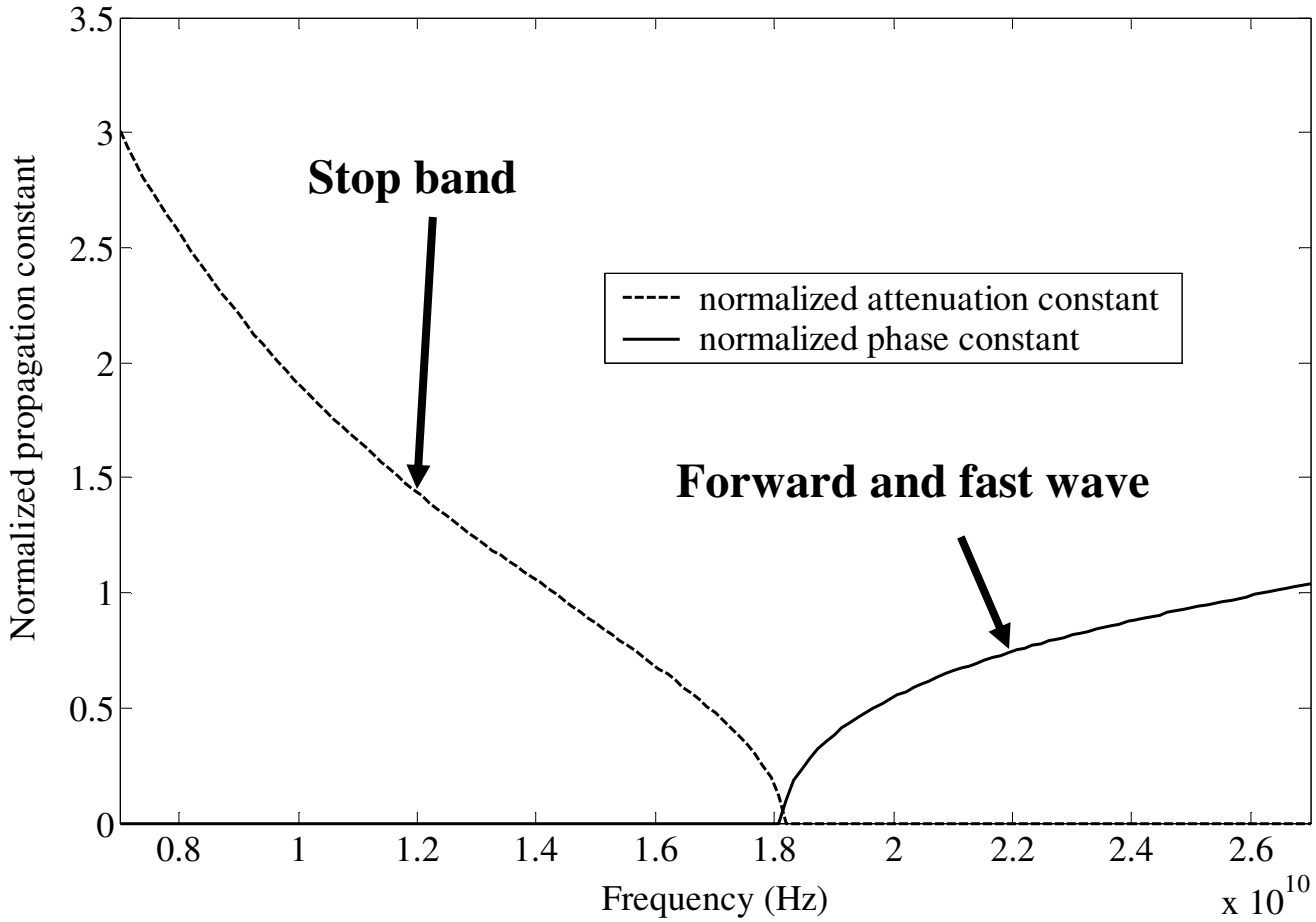

Ring FSS slot printed periodic waveguide

Normalized wave impedance (Z/Z_0)

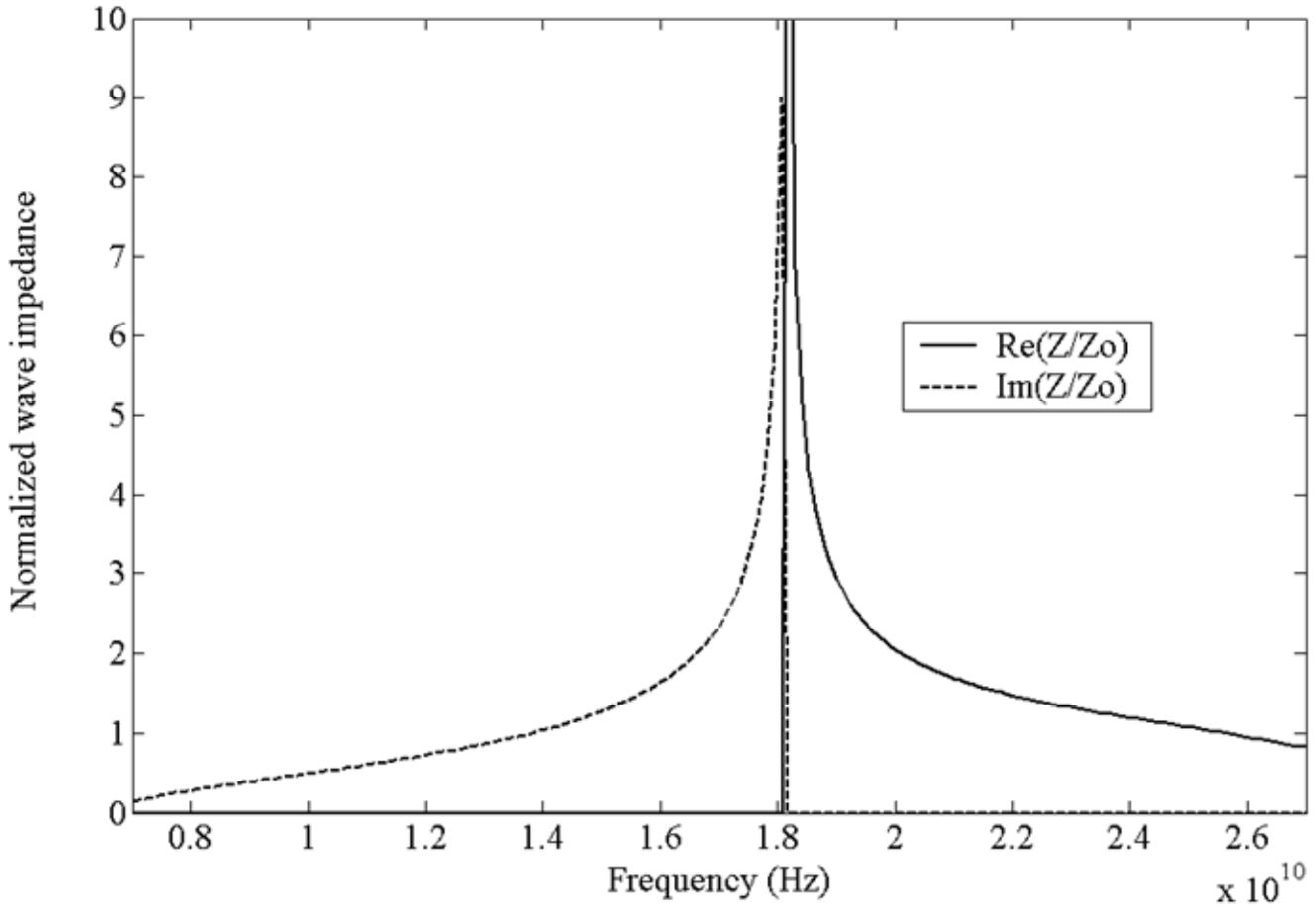

Section 3

Applications

Stepped Impedance Slot (SIS) Resonator

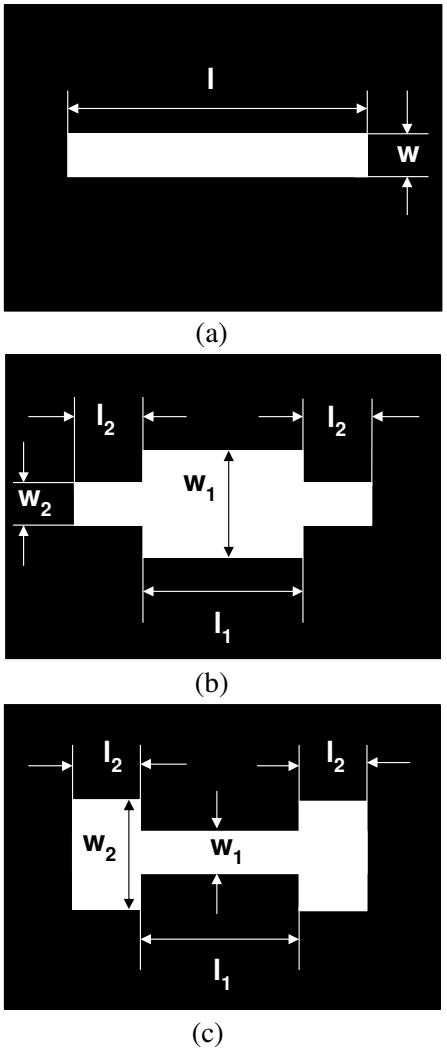

(a) Uniform Impedance Slot (UIS) resonator
(b) SIS resonator I
(c) SIS resonator II

Aim is to explore such SIS resonators to increase the frequency band stop between the fundamental f_r and spurious harmonic f_s resonant frequencies

UIS Resonator

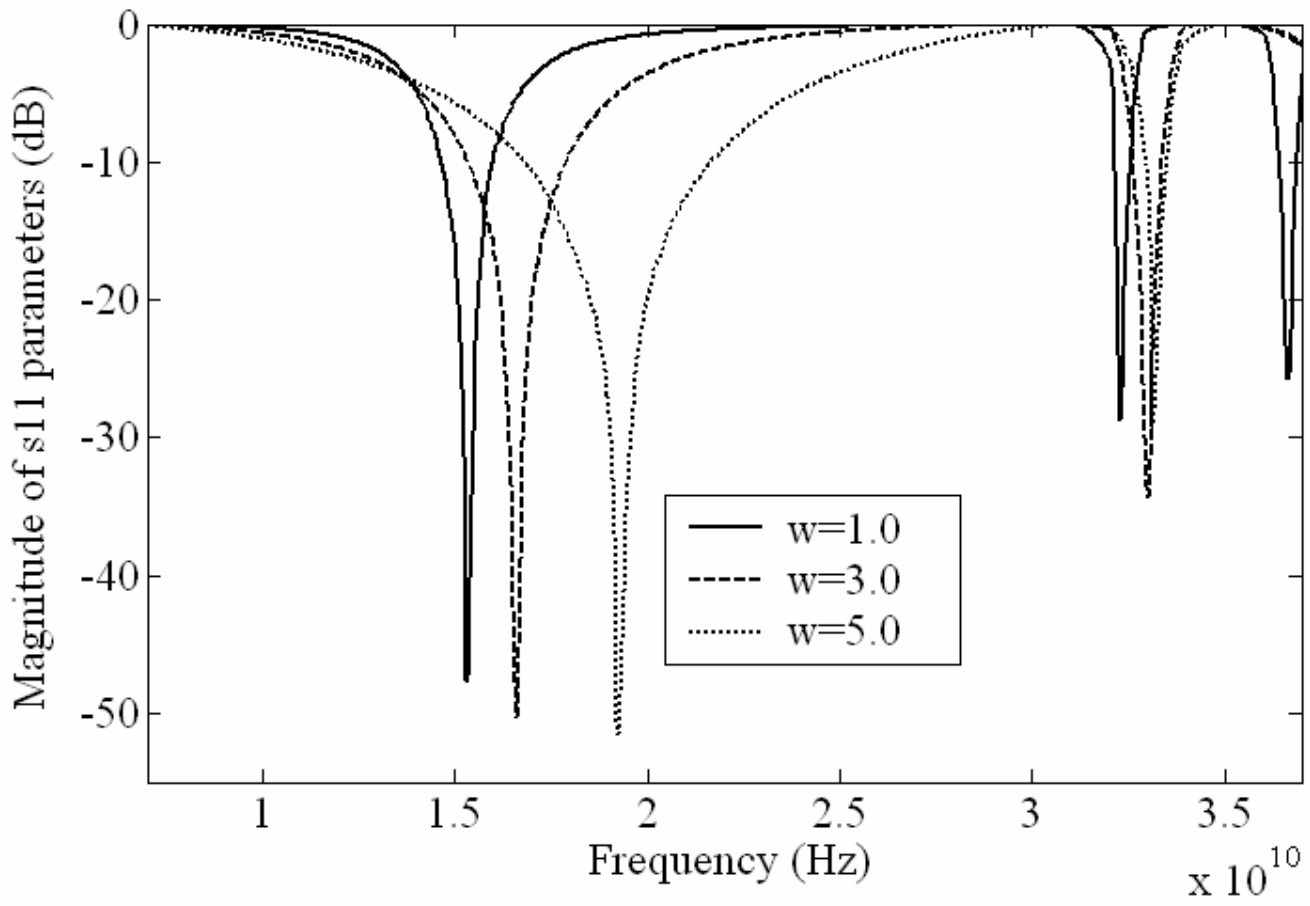

UIS Resonator (Contd.)

- Length of this UIS resonator is kept fixed (l=10.0mm) whereas width is varied from w=1.0mm, 3.0mmm and 5.0mm.
- It can be inferred from previous Figure that fundamental resonant frequency f_r increases as the width of UIS resonator increases whereas there is only slight change in spurious harmonic resonant frequency f_s thereby decreasing the (f_s-f_r) frequency bandstop.
- The maximum fractional stopband width occurs when w=1.00mm [(f_s-f_r) /f_r=(32.2-15.30)GHz/15.3GHz=1.10].
- Is it possible to increase this frequency band stop further?

SIS Resonator I

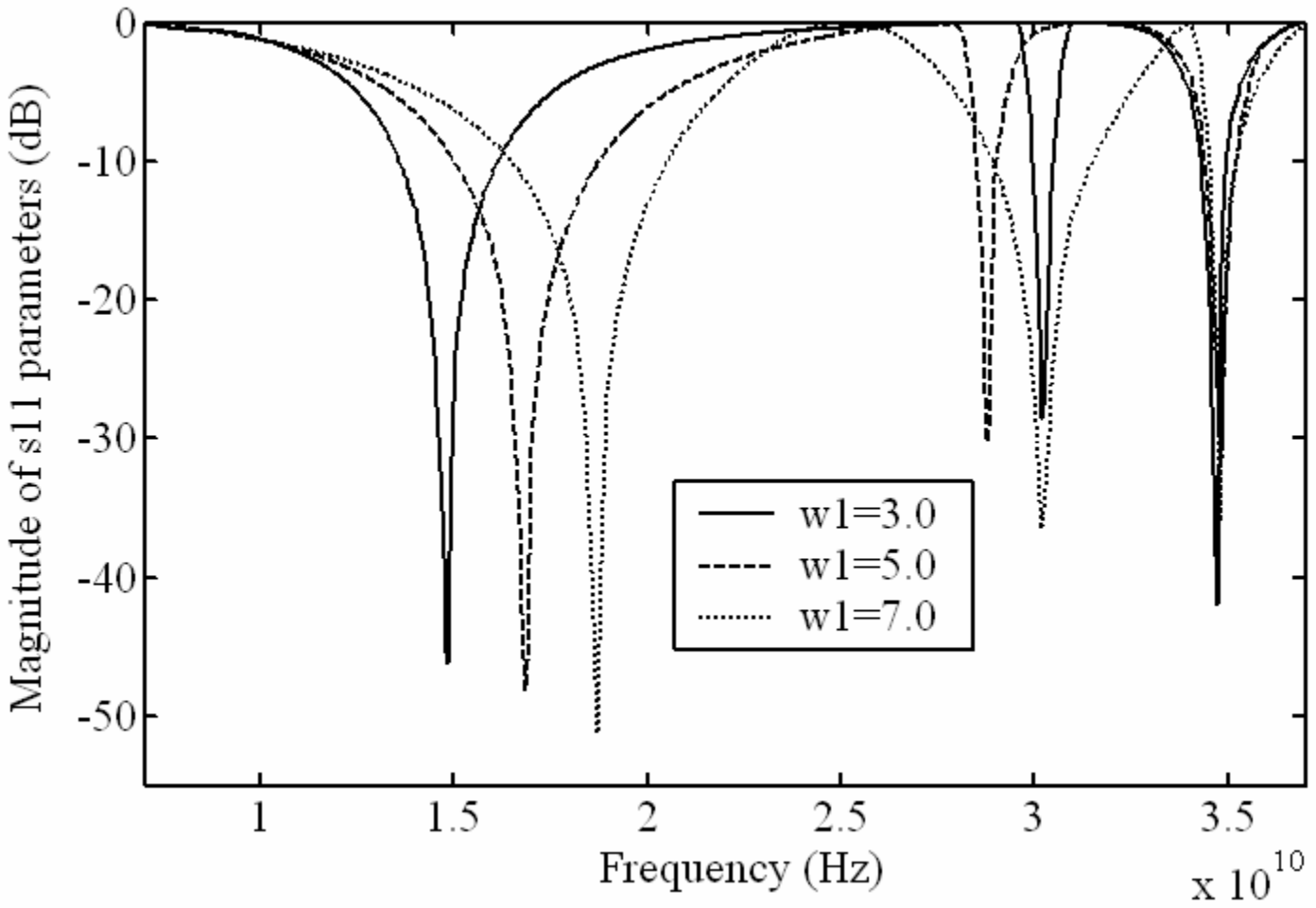

SIS Resonator I (Contd.)

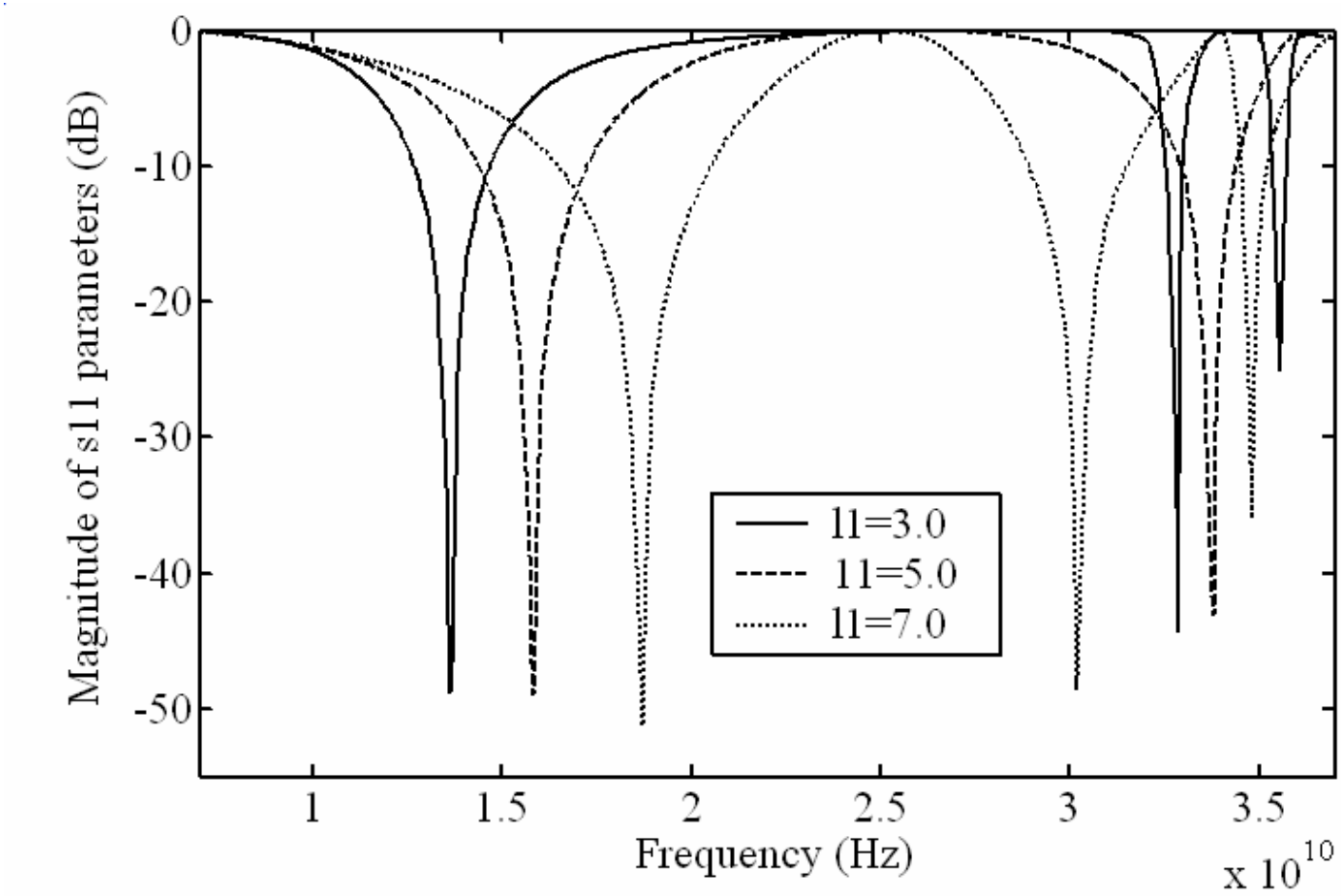

SIS Resonator I (Contd.)

- The main parameters which affect the performance for such slot resonator are w_1 and l_1
- As w_1 increases from 3.0mm, 5.00mm and 7.00mm, the fundamental resonant f_r increases and the (f_s-f_r) frequency bandstop decreases. When w1=7.00mm, minimum fractional stopband width is achieved $[(f_s-f_r)/f_r=(30.25-18.7)GHz/18.7GHz=0.617]$.
- As l_1 increases from 3.00mm, 5.00mm and 7.00mm fundamental resonant frequency f_r increases and f_s decreases, consequently decreasing the (f_s-f_r) frequency stopband.
- When l_1=7.00mm, minimum fractional stopband width is achieved $[(f_s-f_r)/f_r=(30.2-18.7)GHz /24.45GHz=0.47]$.
- Hence, SIS resonator I basically decreases the frequency band stop.

SIS Resonator II

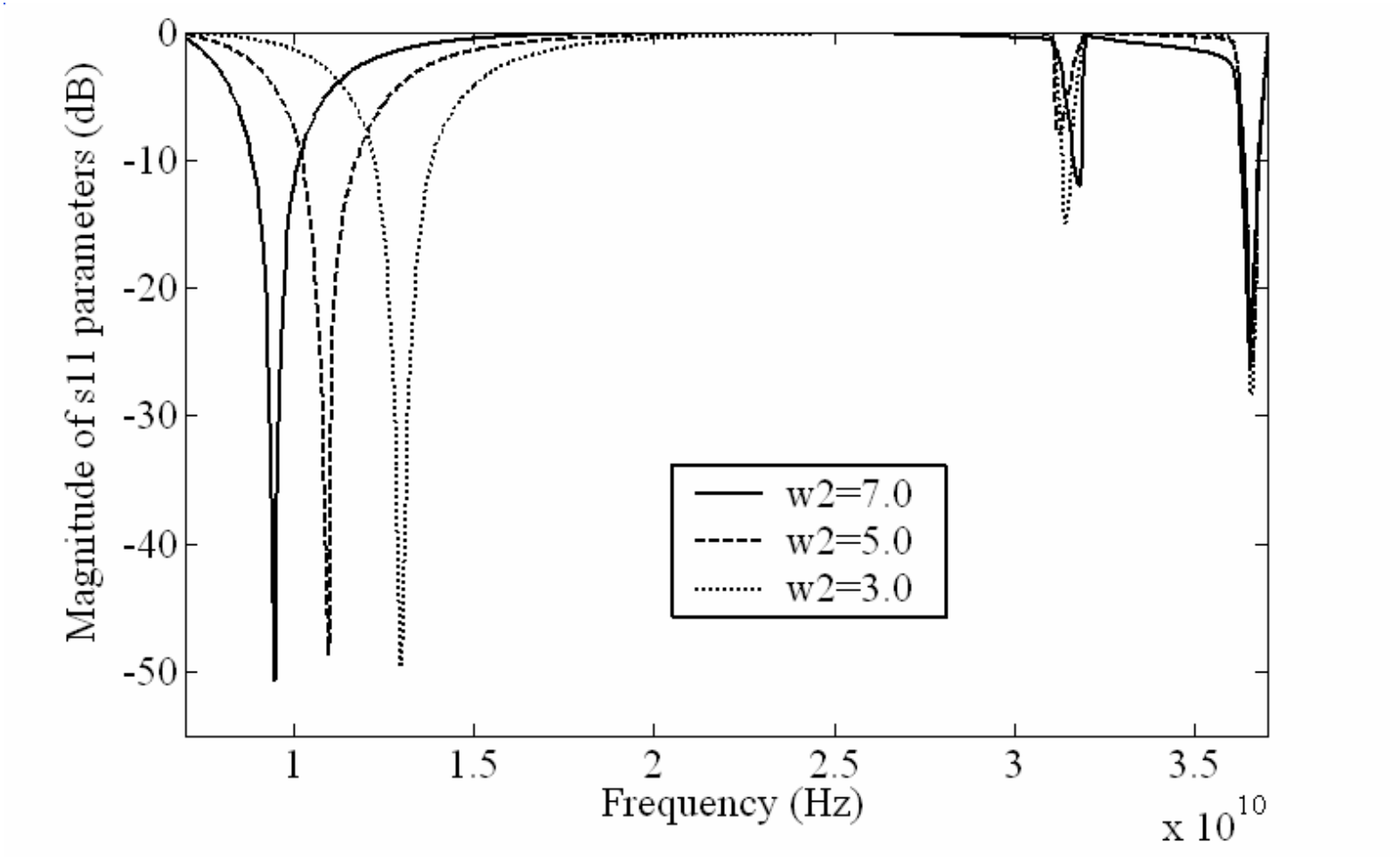

SIS Resonator II (Contd.)

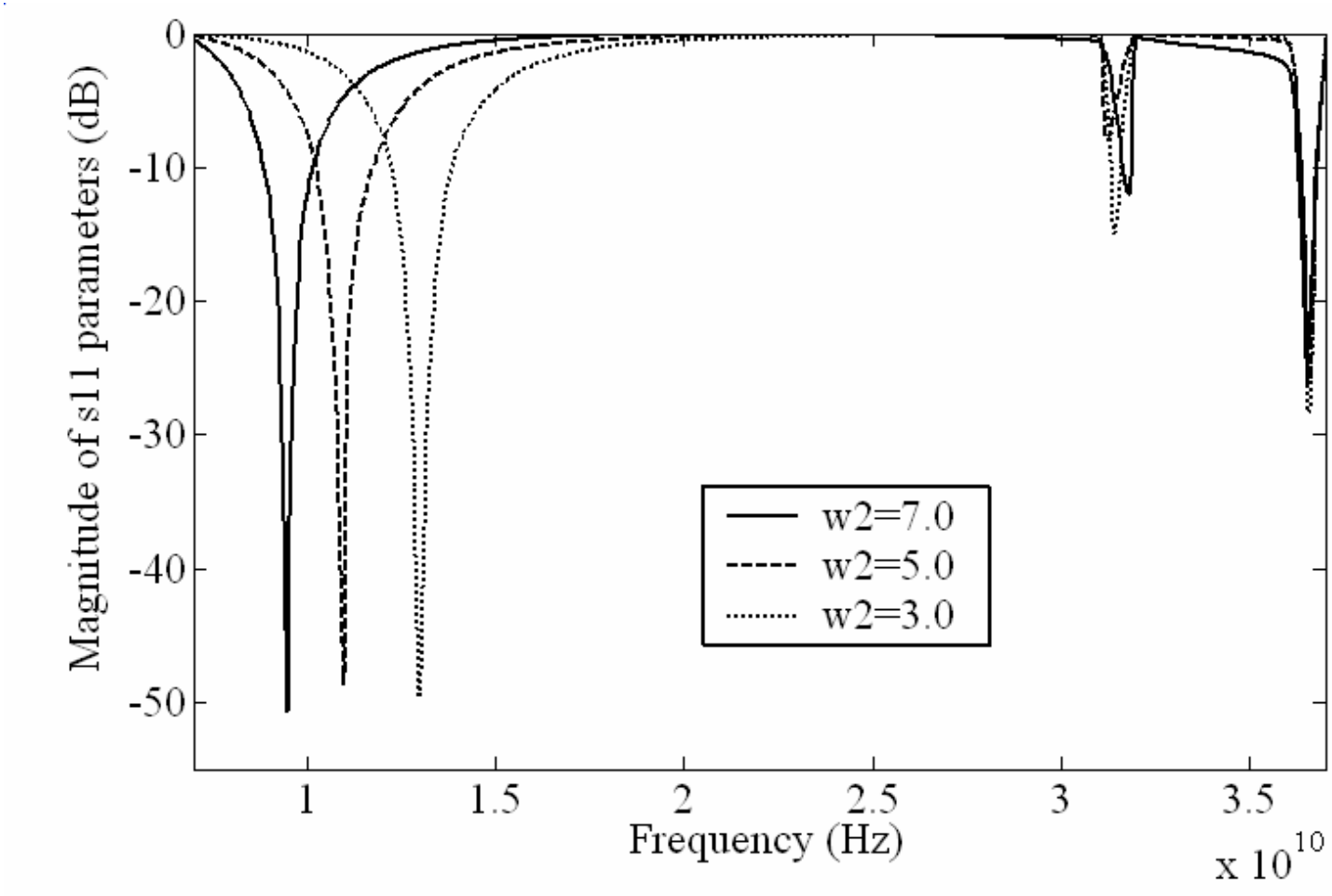

SIS Resonator II (Contd.)

- As w_2 increases from 3.0mm, 5.00mm and 7.00mm, fundamental resonant frequency f_r further decreases and the (f_s-f_r) frequency bandstop increases.
- The maximum fractional stopband width is $[(f_s-f_r)/f_r=(31.8-9.5)GHz/9.5GHz=2.34]$ when $w_2=7.00mm$.
- As l_1 increases from 3.00mm, 5.00mm and 7.00mm fundamental resonant frequency f_r decreases and the (f_s-f_r) frequency bandstop increases.
- When $l_1=7.00mm$, maximum fractional stopband width is achieved $[(f_s-f_r)/f_r=(36.2-8.7)GHz/22.45GHz=1.22]$.
- Further optimization is also possible for enhancing the maximum fractional stopband width by properly adjusting the aspect ratio of w_2, w_1 and the dimension of l_1.

Harmonic suppressed waveguide band pass filters

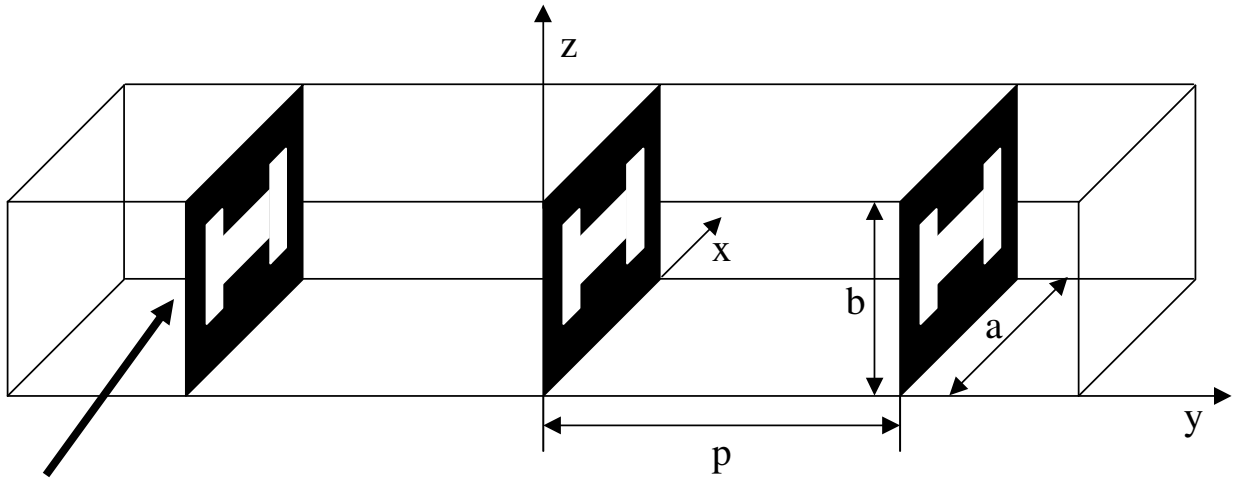

SIS Resonators II

3-D Geometry

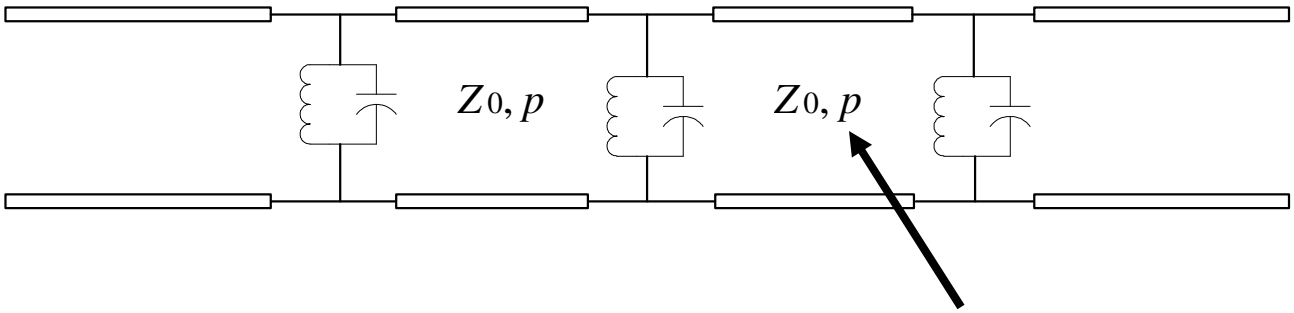

Eqt. Ckt. Network

p ≈$\lambda_g/4$

Harmonic suppressed waveguide band pass filters (Contd.)

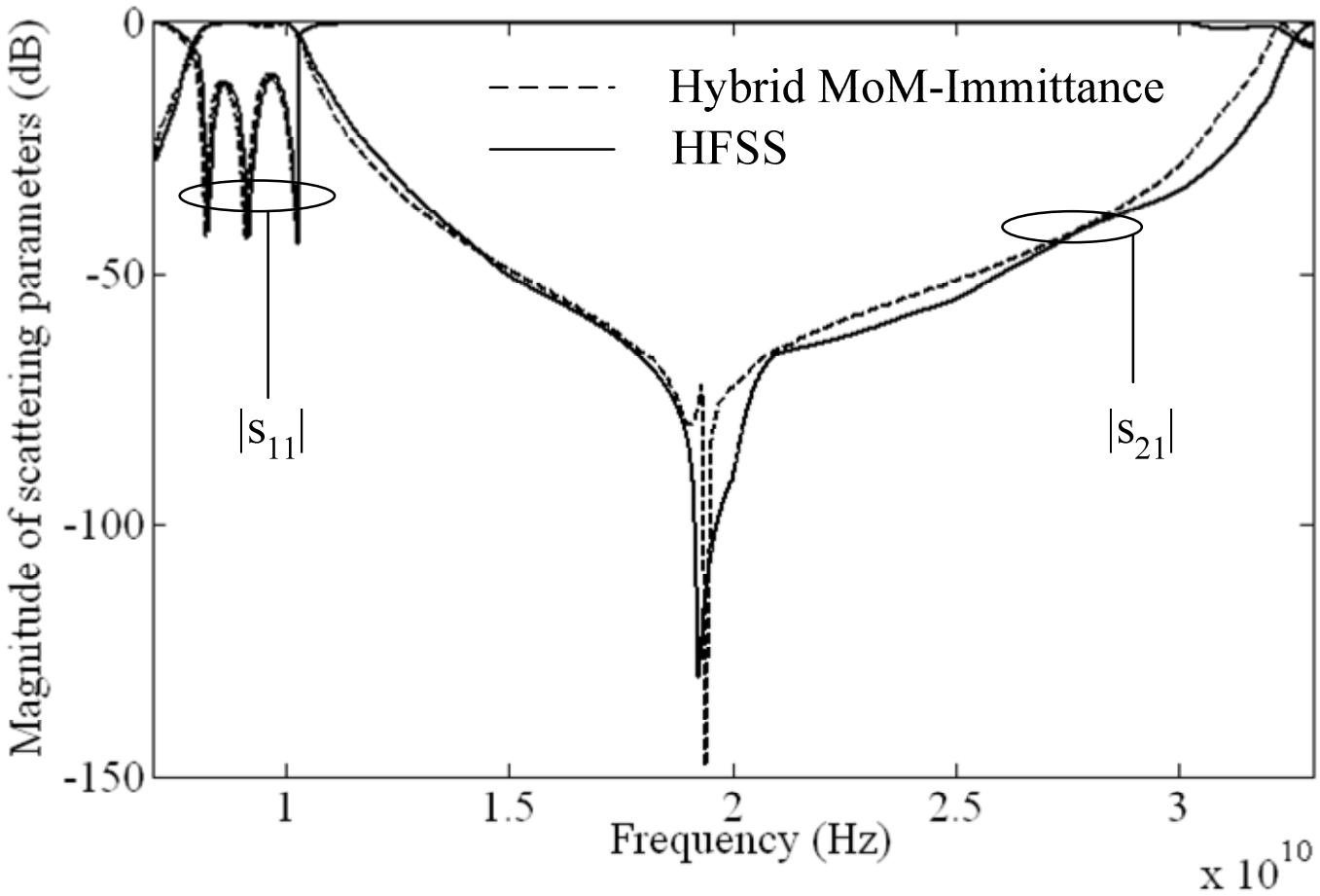

Harmonic suppressed waveguide band pass filters (Contd.)

- Optimized value is p=8.23mm for the chosen dimensions of SIS resonators II (w_1=1.0mm, w_2=9.0mm, l_1=3.0mm and l_2=3.5mm).
- Designed waveguide band pass filter achieves a bandwidth of 23.8% for return loss < -10dB at mid-band frequency of 9.3GHz.
- Out-of-band rejection bandwidth is increased extensively (~23GHz) and mid-stop band attenuation is significantly reduced to less than -100dB at approximately 19.4 GHz.
- Furthermore, frequency response at the two sides of passband becomes much steeper than conventional band pass filters.

Waveguide based EBG

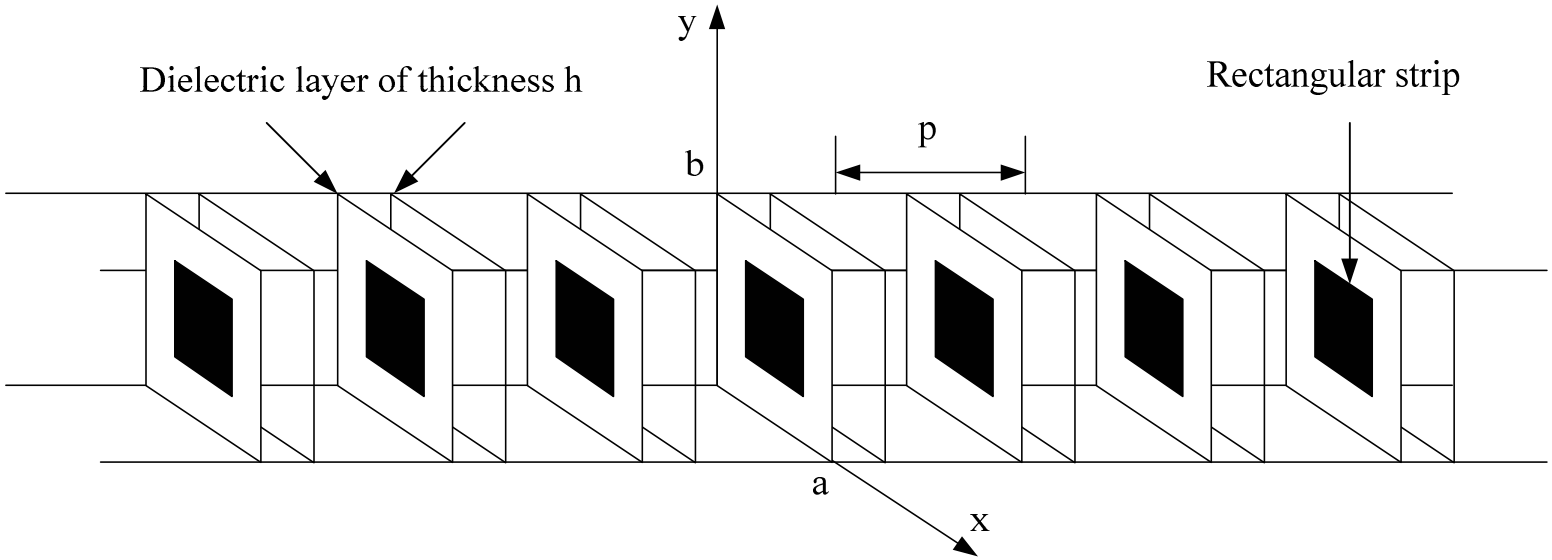

A finite periodic waveguide structure loaded with units/cells of printed strips of l=9.0mm and w=3.0mm and printed on dielectric layer of thickness h=1.0mm of periodicity p inside an X-band waveguide has been investigated.

Waveguide based EBG (Contd.)

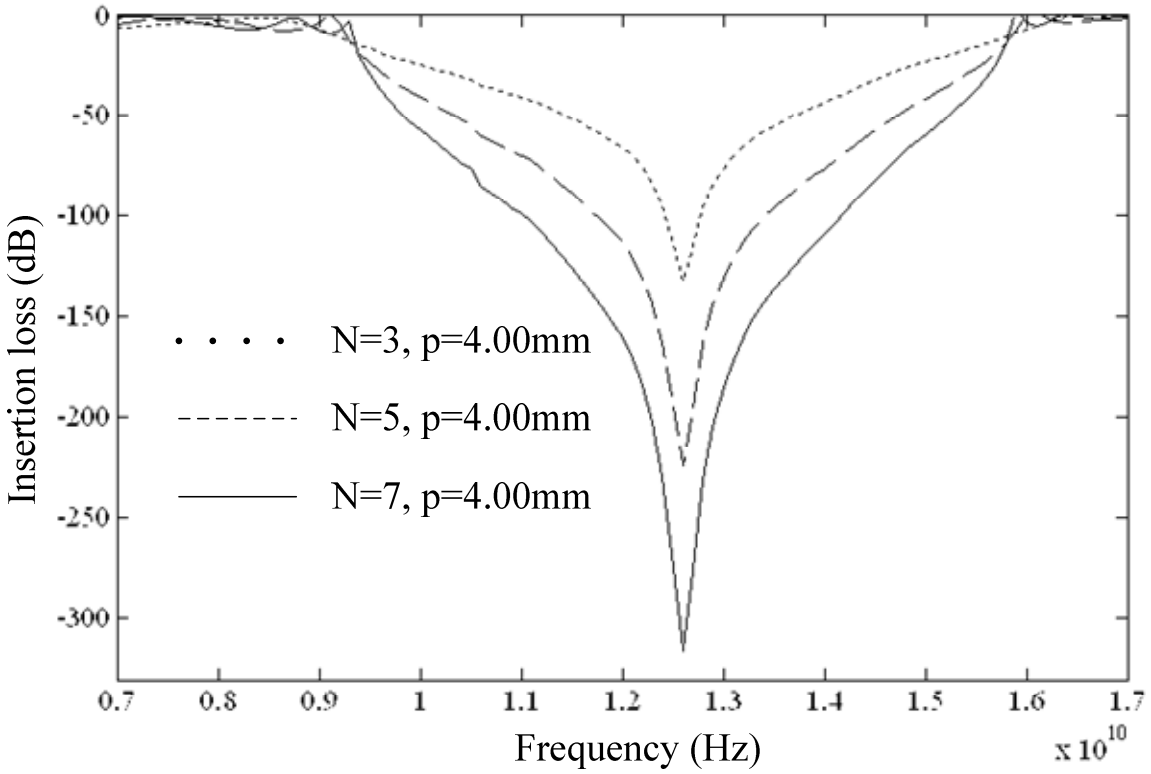

Effect of the number of periods on the EBG: As number of unit cells (N) increases, insertion loss goes into deep rejection band as mentioned in many literatures

Waveguide based EBG

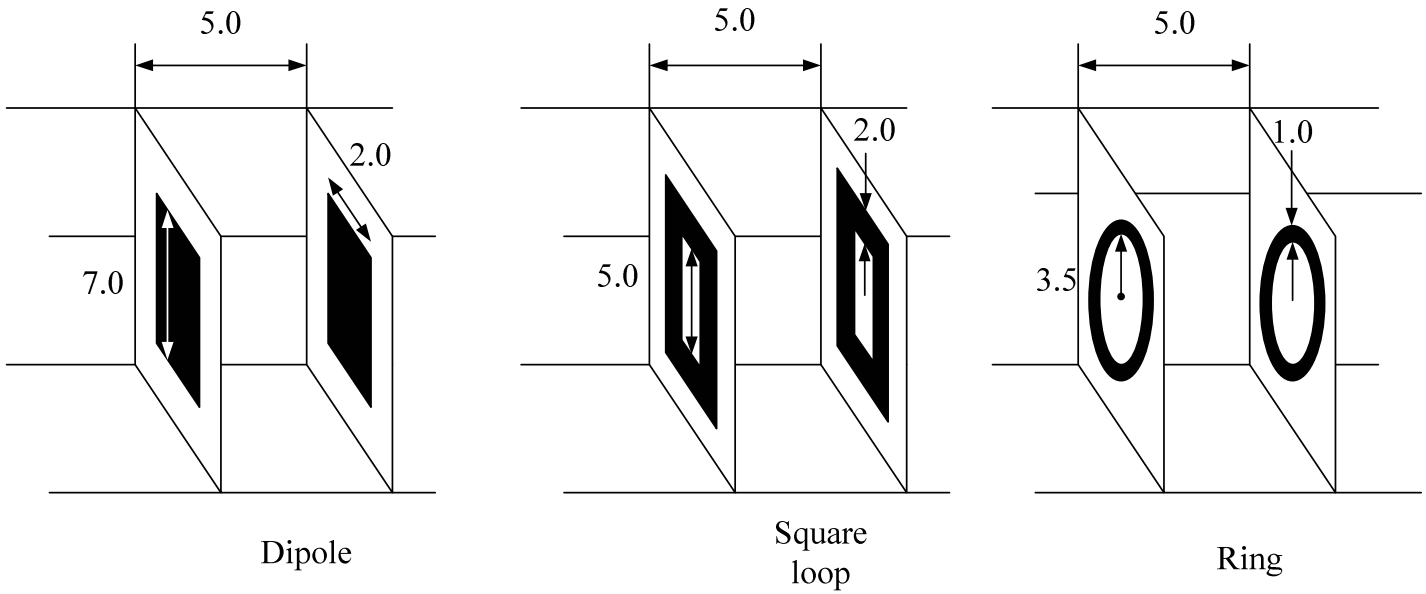

Let us investigate which FSS strip loaded waveguide structure has the widest EBG.

Waveguide based EBG (Contd.)

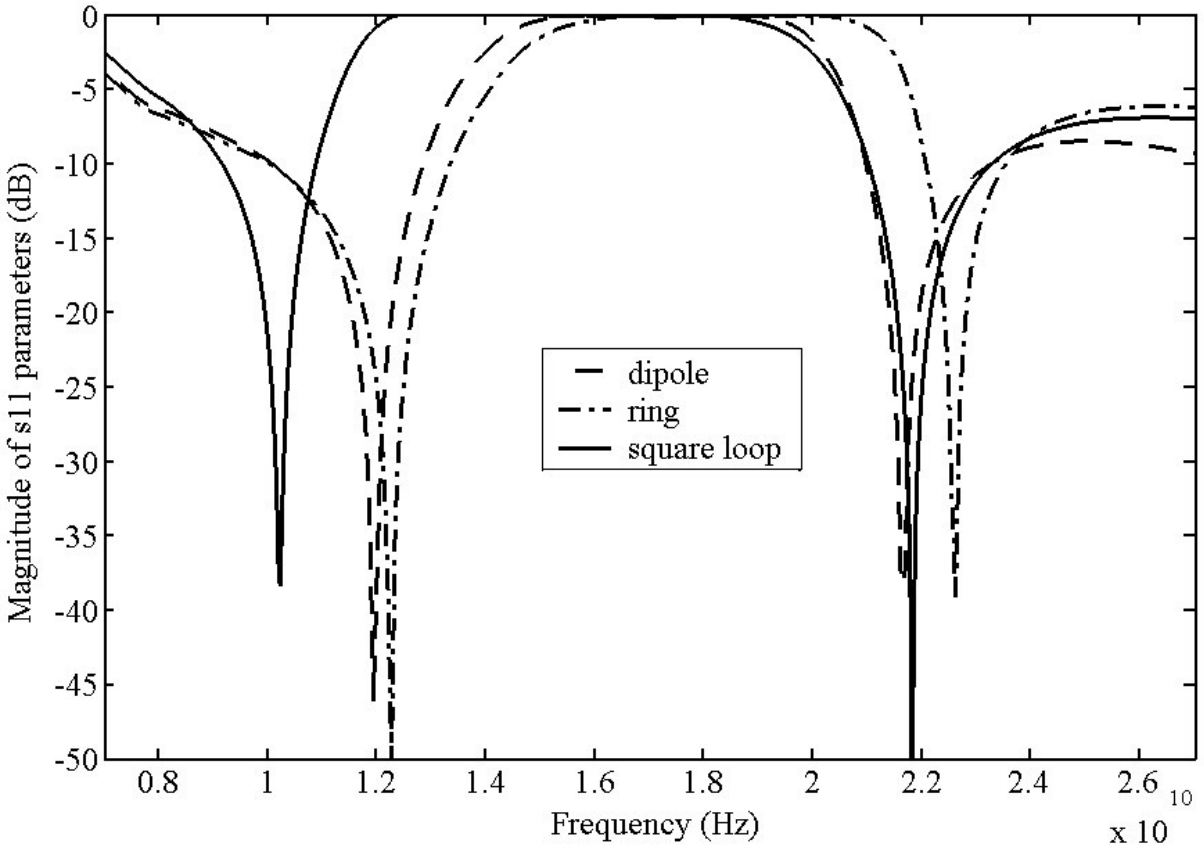

As we can observe, the square loop FSS strip has the widest EBG hence let us optimize this structure for designing a wideband EBG structure.

Waveguide based EBG (Contd.)

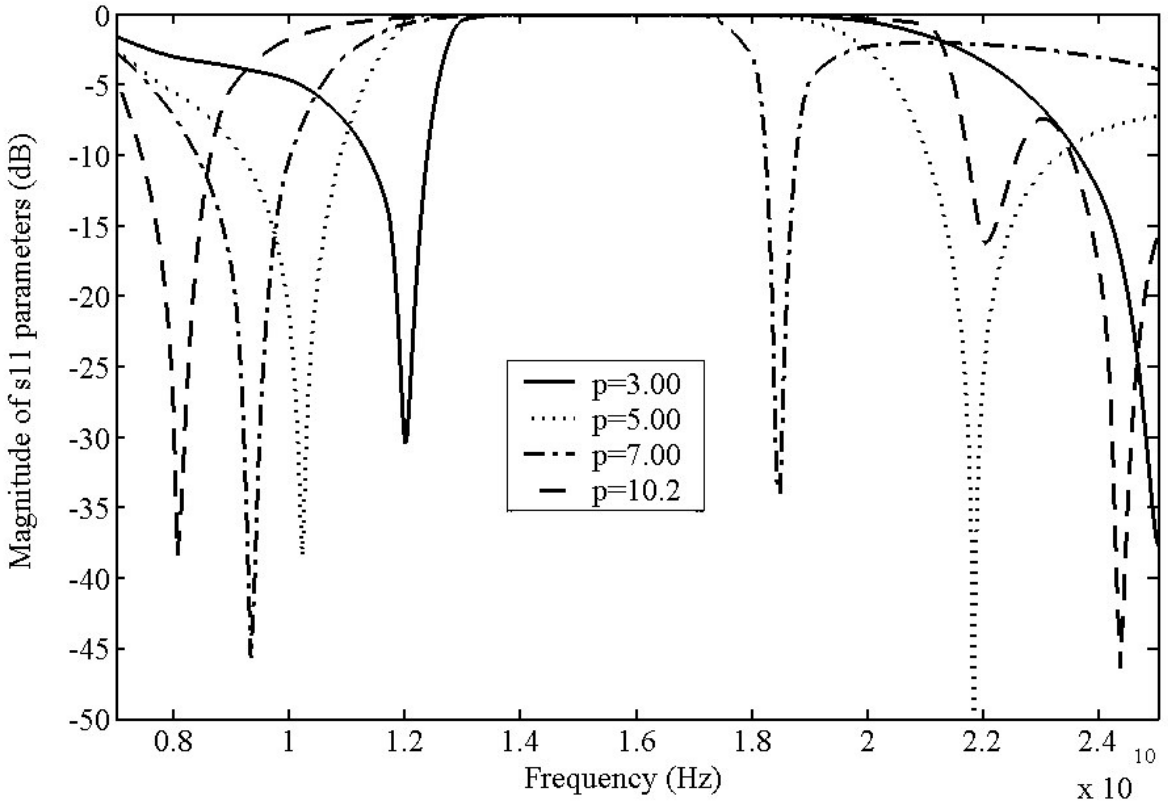

Effect of periodicity: There is a downward frequency shift in bandstop as periodicity p is increased from p=3.00mm, 5.00mm, 7.00mm and 10.2mm. Besides, there is visible enhanced bandwidth for periodicity of p=10.2mm in comparison to other values of p.

Waveguide based wideband EBG

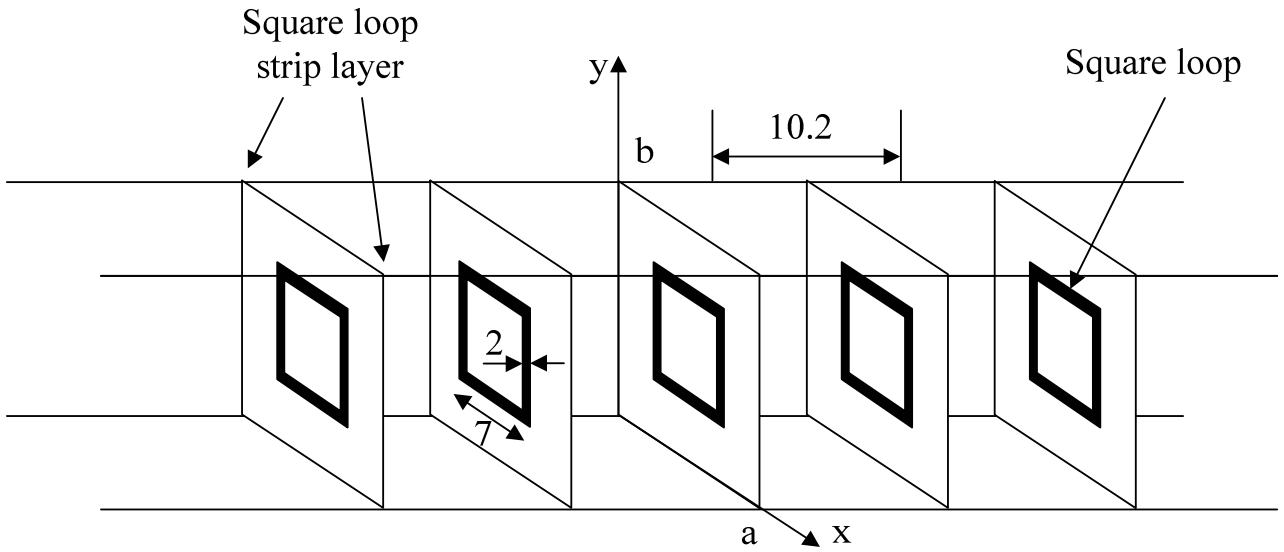

3-D Geometry

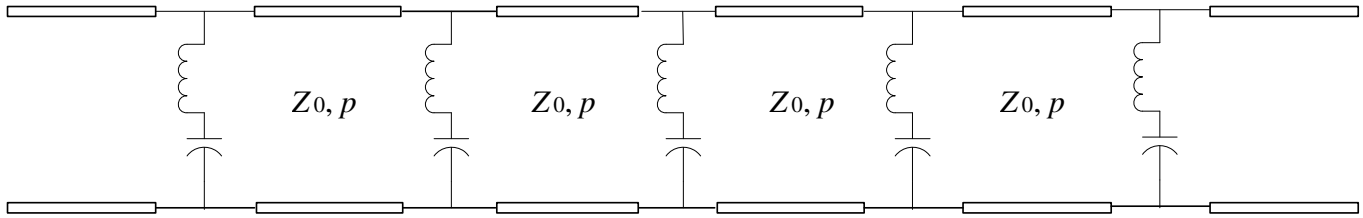

Eqt. Ckt. Network

Waveguide based EBG (Contd.)

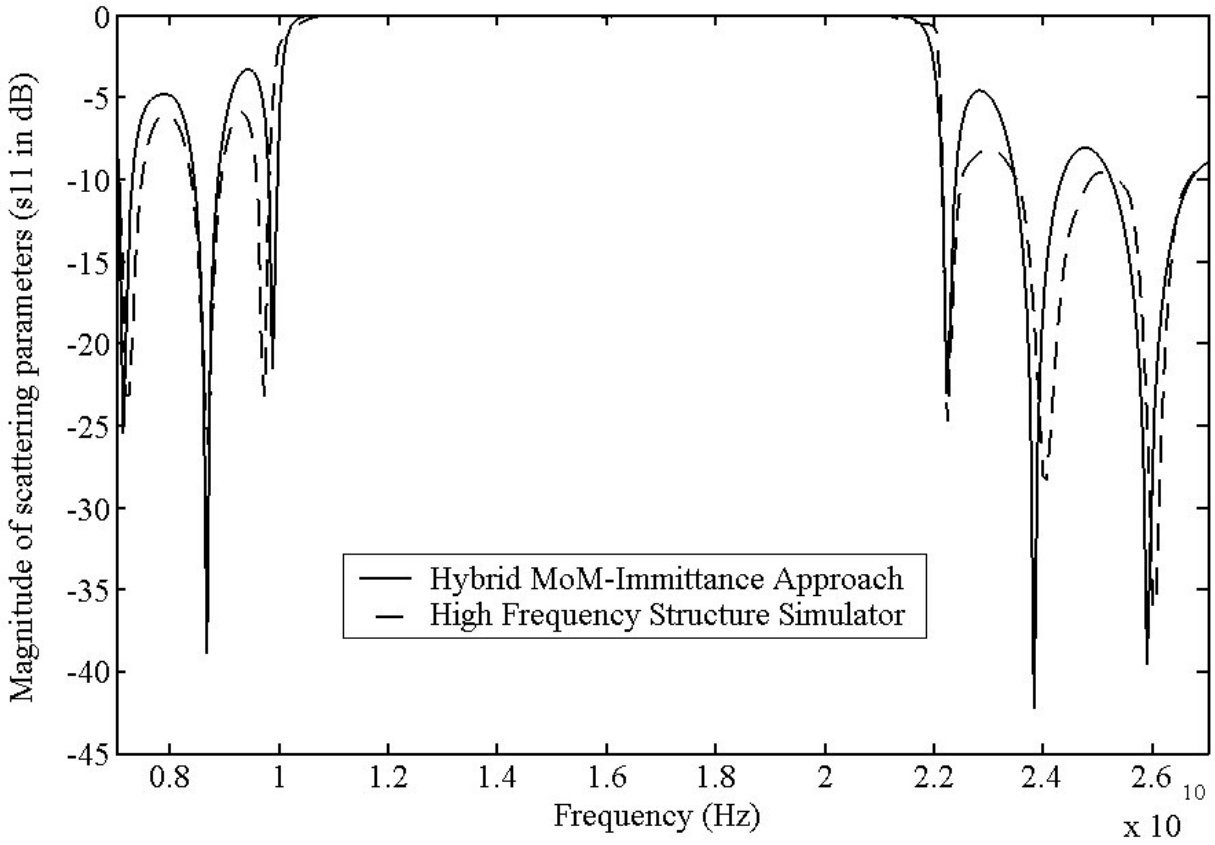

It can be observed that there exists EBG or forbidden band with $|S_{11}|$ of about 0dB in frequency region from 10.5GHz to 21.5GHz.

Simple Architecture for Waveguide based DNG Metamaterials

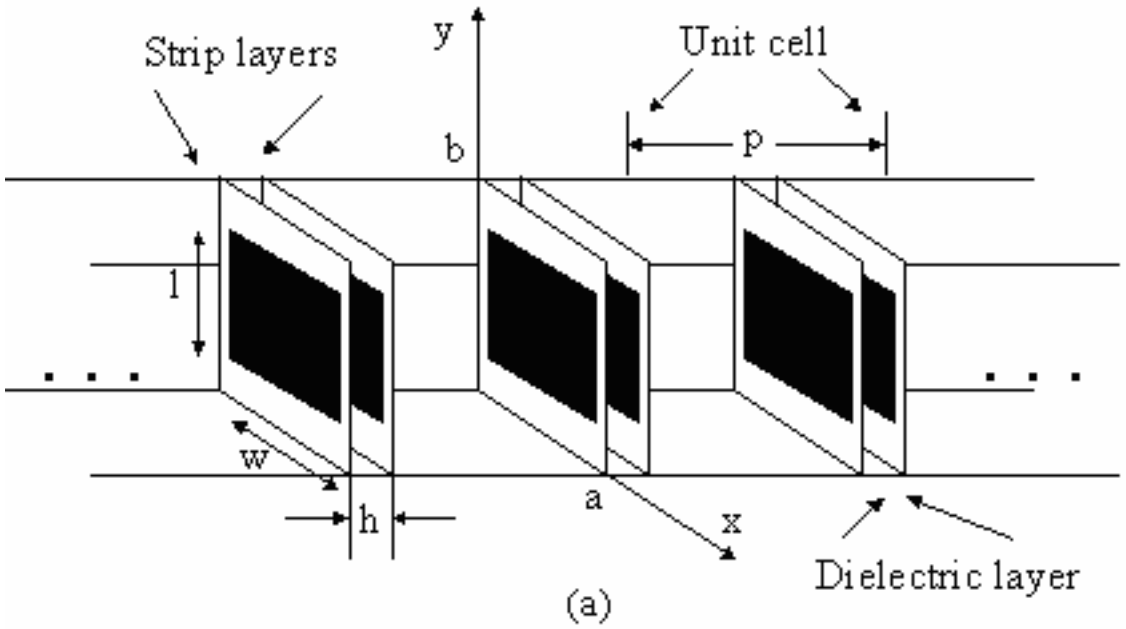

(a)

Parameters	w	l	h	p	
Case I	8.00 mm	6.00 mm	1.00 mm	3.00mm	3.78
Case II	8.00 mm	6.00 mm	2.00 mm	3.00mm	3.78
Case III	8.00 mm	6.00 mm	1.00 mm	3.00mm	7.00

Simple Architecture for Waveguide based DNG Metamaterials

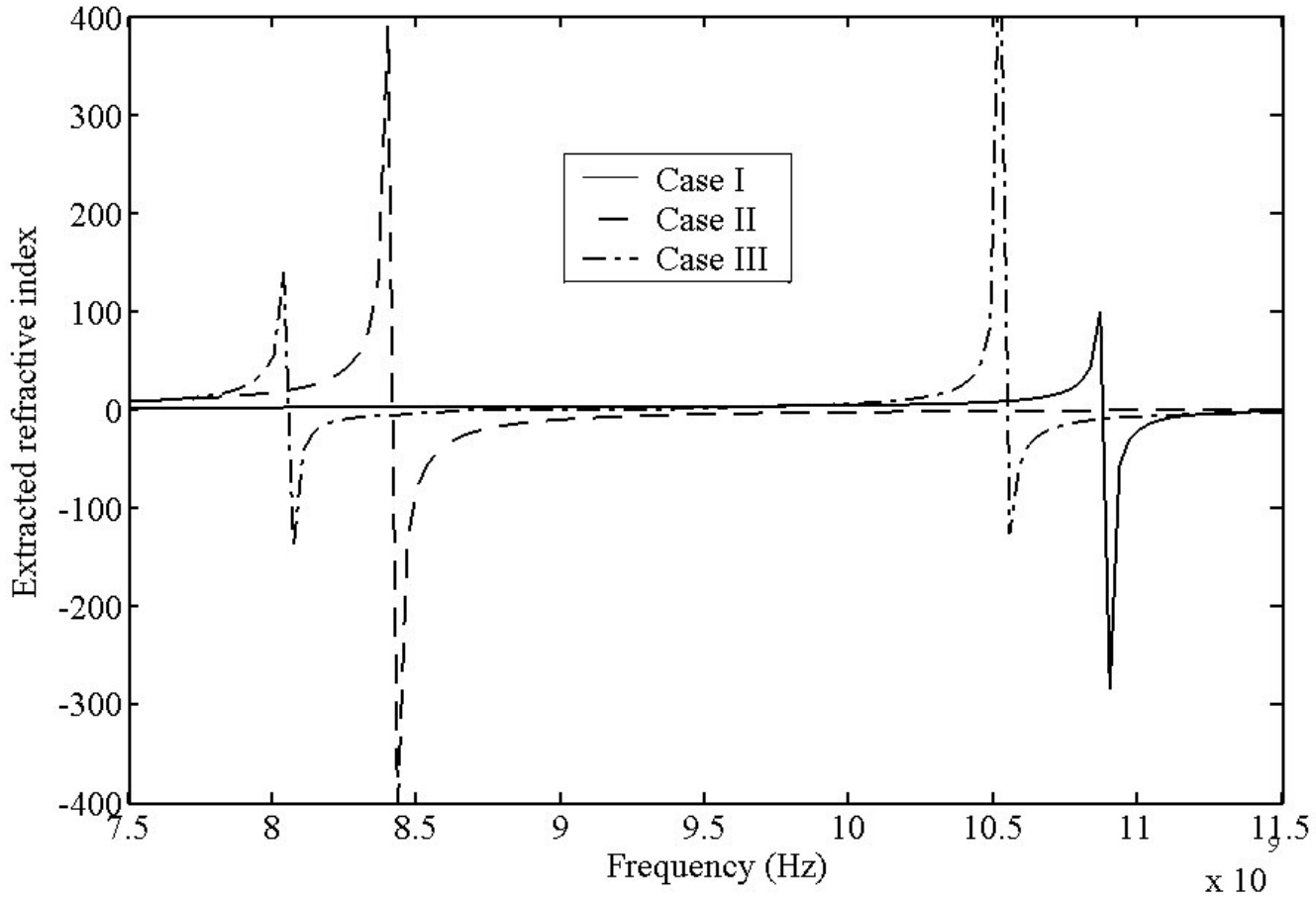

Simple Architecture for Waveguide based DNG Metamaterials

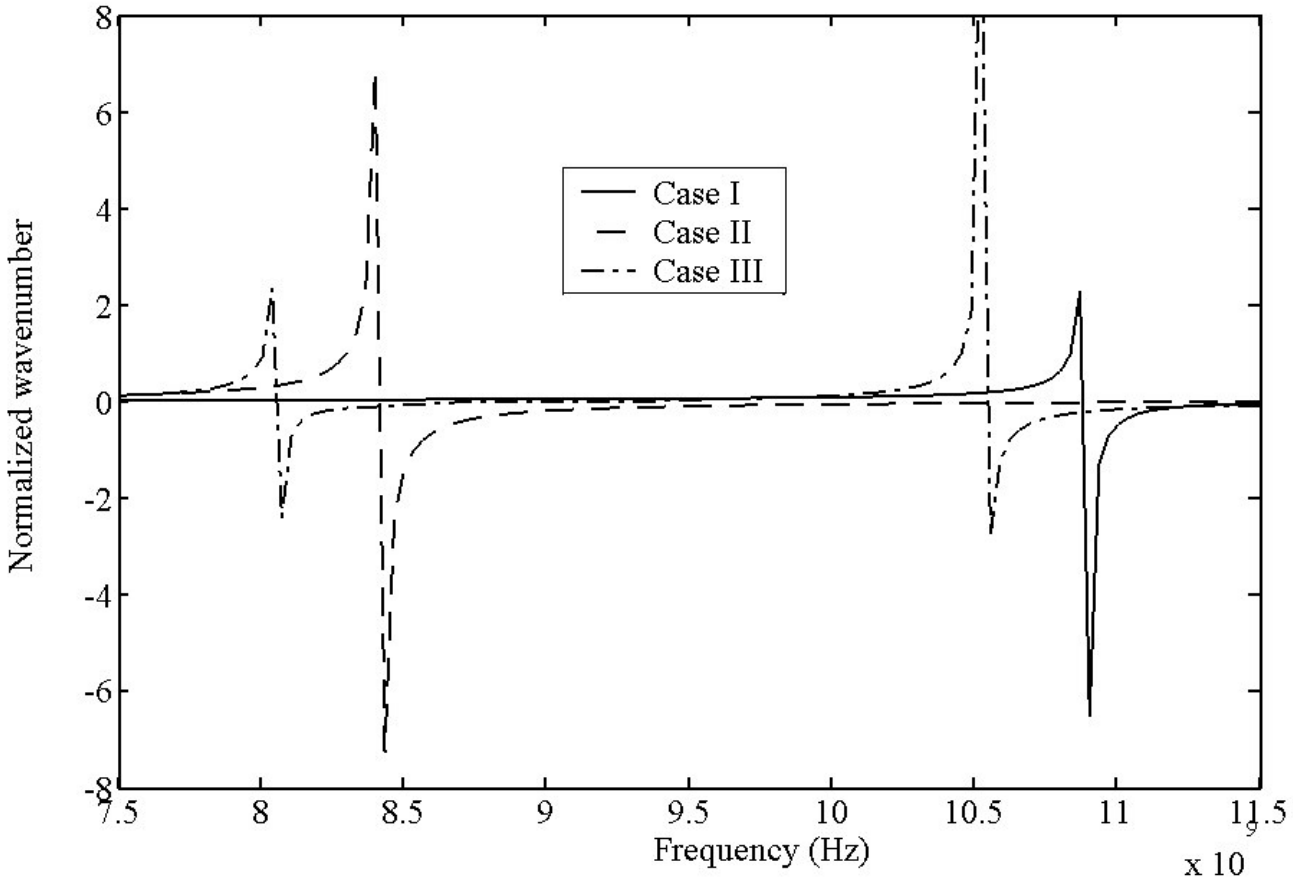

Conclusions

- A hybrid numerical method has been developed for full-wave characterization of printed strips and slots. This method is hybrid of three basic numerical methods viz., MoM, Immittance approach and Mode-matching method.
- From the full-wave characterization of a single unit/cell, per-unit length transmission parameters or guided-wave characteristics for printed periodic waveguide structures loaded with various FSS elements has been numerically obtained and studied for various applications.
- Harmonic suppressed waveguide band pass filters has been designed using SIS resonators coupled by $\lambda/4$ waveguide impedance transformers.
- Wideband waveguide based EBG/PBG structures has been investigated for the effect of various parameters like periodicity, number of periods and FSS strips.
- A simple architecture for waveguide based DNG metamaterials has been proposed. Double printed periodic waveguide structures exhibit the fundamental properties of metamaterials like backward wave, negative ε and μ, negative index of refraction.

Future Works

- In this work we have assumed that the metal/strip is infinitely thin.
- Lossy effects has been neglected.
- For periodic analysis, we have assumed that the all modes are localized which may not be correct for the periodic waveguide structures with small periods.
- We can explore the printed periodic waveguide structures with the fast wave for designing fast-wave feeding lines for applications in the leaky wave antennas.
- Doing some experiments for the periodic waveguide based devices

Publications

Journal Papers

- R. S. Kshetrimayum and L. Zhu , "Hybrid MOM-Immittance approach for full-wave characterization of printed strips and slots in layered waveguide and its applications," IEICE Trans. On Electronics*: Special Section on Measurement Technologies for Microwave Materials, Devices and Circuits*, Vol. E87-C, No. 5, pp. 700-707, May 2004.
- R. S. Kshetrimayum and L. Zhu , "Guided-wave Characteristics of Waveguide Based Periodic Structures Loaded with Various FSS Strip Layers," accepted for publication in IEEE Trans. on Antennas and Propagation*: Special Issue on Artificial Magnetic Conductors, Soft/Hard Surfaces, and other Complex Surfaces*, Jan. 2005.
- R. S. Kshetrimayum, "A Brief Introduction to Metamaterials," accepted for publication in IEEE Potentials (Dec. 2004/Jan. 2005 issue).
- Submitted to IEEE MWCL, MOTL, IJRFMiCAE and IEE Proc. MAP.

Publications

Conference Papers

- R. S. Kshetrimayum and L. Zhu, "Multimode Network Equivalence of Waveguide Discontinuities using full-wave Method of Moments for Spatial Power Combining System," in Proc. PIERS, January 7-10, 2003, Singapore, pp. 72.
- R. S. Kshetrimayum and L. Zhu, "Equivalent Circuit Model of Planar Strips in Layered Waveguide for Synthesis Design of Printed Periodic Waveguide Structures," in Proc. APMC, Nov 4-7, 2003, Seoul, South Korea, pp. 471-474.
- R. S. Kshetrimayum and L. Zhu, "A Novel Waveguide Based Metamaterials," Proc. ISAP, Aug 17-21, 2004, Sendai, Japan, pp. 469-472.
- Exhibitions/Talks on metamaterials at COE Tech Week, Institute of Materials (East Asia), etc.

Have a peaceful day.

Thanks!